# FINAL TECHNICAL REPORT

# Comparative Analysis of Fluid Inclusion Geochemistries from World-Class and Small-Scale Zn-Pb Deposits in the Ozark Plateau using Laser Ablation ICP-MS and Raman Spectroscopy

**U.S. Geological Survey Mineral Resources External Research Program**

Award Number: 06HQGR0178

Principal Investigator: Martin S. Appold

Department of Geological Sciences
University of Missouri—Columbia
Columbia, MO 65211

October 9, 2009

Research supported by the U.S. Geological Survey (USGS), Department of the Interior, under USGS award number 06HQGR0178. The views and conclusions contained in this document are those of the authors and should not be interpreted as necessarily representing the official policies, either expressed or implied, of the U.S. Government.

## Abstract

Fluid inclusions hosted by sphalerite and dolomite and quartz gangue from the Southeast Missouri, Tri-State, and Northern Arkansas Mississippi Valley-type (MVT) districts of the Ozark Plateau of the central U.S. were analyzed using laser ablation inductively coupled plasma mass spectrometry (LA-ICP-MS) and Raman spectroscopy. The goals of the study were to characterize the chemical composition of fluids involved in mineralization. In particular, the study aimed to determine the ore metal and sulfur concentration, pH, and redox potential of the mineralizing fluids, to identify the mechanisms that caused the precipitation of the ores, and to determine if any compositional differences existed between fluids that deposited giant MVT districts like Southeast Missouri and Tri-State compared to those that deposited a small district like Northern Arkansas.

The results of the study showed that the MVT deposits in each district were deposited from brines with similar overall geochemistry dominated by the cations, Na, Ca, K, Mg, Sr, and Ba. Each of the three districts had a population of sphalerite-hosted fluid inclusions that was anomalously Pb and Cu rich relative to typical sedimentary basinal brines, with concentrations on the orders of 100's to 1000's of ppm. Gangue mineral-hosted fluid inclusions did not have ore metal concentrations above the detection limits of 1's to 10's of ppm. These results point to the invasion of a metal rich brine during the time of sulfide mineral precipitation. The high metal concentrations would have prevented simultaneous transport of large concentrations of sulfide. Thus, MVT ore deposition is more likely to have been caused by mixing of a metal rich fluid with a $H_2S$ rich fluid or mixing of a fluid carrying metals and sulfate with another fluid rich in a reductant like methane. A constraint on the relative likelihood of these two mechanisms may come from the gas geochemistry of the fluid inclusions. Methane is prevalent in fluid inclusions in both sphalerite and gangue minerals from all three districts suggesting reducing log $f_{O_2}$ values in the range of about $-54$ and $-55$ , whereas $H_2S$ is present only in sphalerite-hosted fluid inclusions. This suggests that sulfur was transported with metals, most likely in the form of sulfate, which was reduced to sulfide, perhaps by methane, in the reducing environment encountered in the MVT districts, triggering sulfide mineral precipitation.


## Statement of Problem

Mississippi Valley-type (MVT) deposits represent some of the greatest enrichments of zinc and lead in the Earth's crust, exceeding average crustal concentrations by as much as three orders of magnitude in deposits up to hundreds of millions of tons in size. Several decades of research has produced a general model for MVT ore formation involving precipitation from sedimentary brines that commonly were set in motion by tectonic activity. However, many important details of MVT ore formation have remained unclear, such as exactly what causes the ores to precipitate from the brines. Possible precipitation mechanisms that have been proposed can be grouped into three categories (Sverjensky, 1986):

(1) Reduced sulfur model: Ore metals and sulfide are transported together in solution with sulfide mineral precipitation caused by cooling, dilution, or pH increase.

(2) Sulfate reduction model: Ore metals are transported in solution with sulfate, which is reduced to sulfide at the site of ore deposition most likely by organic matter.

(3) Mixing model: Ore metals and sulfide are transported in separate fluids that mix at the site of ore deposition.

Some of the most powerful clues to the answer to the precipitation mechanism question lie in the ore fluid composition. The major element composition and temperature of MVT ore fluids have long been known. However, other ore fluid characteristics have been much less certain. Chief among these are the ore metal content, the sulfur content, the pH, and the redox potential. Knowledge of these ore fluid characteristics will help answer other fundamental question regarding MVT ore genesis, such as whether MVT ore fluids are anomalous in any respects compared to typical sedimentary brines, and to what extent ore fluid chemistry affects MVT deposit size.

The Ozark Plateau of the Central U.S. is perhaps the world's foremost province of MVT mineralization (Fig. 1). The province contains the world's two largest MVT districts—the Southeast Missouri and Tri-State districts, three much smaller but still formerly commercially significant districts called the Northern Arkansas, Central Missouri, and Washington County districts, and numerous subeconomic occurrences of MVT mineralization. Located within the Mississippi River watershed, the Ozark MVT deposits are among the original defining examples of the MVT deposit class. Thus, research findings for the Ozark deposits have broad implications for the MVT deposit class as a whole.

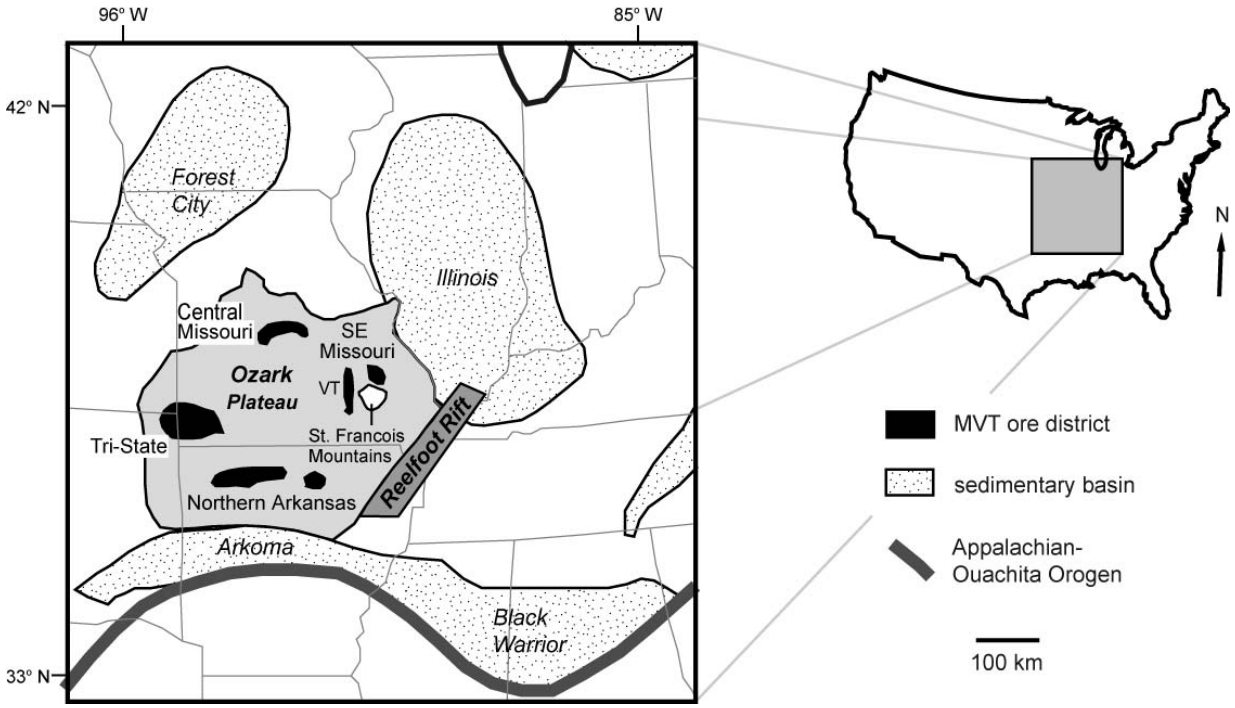


***Figure 1.*** *Map showing the location of the major MVT districts of the Ozark Plateau in relation to other major nearby geologic features (after Appold and Garven, 1999). The Viburnum Trend of the Southeast Missouri district is denoted by "VT."*

## Objectives

The principal objectives of this research project were to answer the following questions:

- What was the composition of the fluids involved in MVT mineralization? In particular, what was their ore metal content?
- What was the sulfur content of the mineralizing fluids?
- What were the pH and redox potential of the mineralizing fluids?
- What precipitation mechanisms were most important in forming the Ozark MVT deposits?
- Did the fluids that formed giant districts like Southeast Missouri and Tri-State differ significantly in composition from those that formed small districts like Northern Arkansas?

These objectives were pursued primarily through the analysis of fluid inclusions using microthermometry, laser ablation inductively coupled plasma mass spectrometry (LA-ICP-MS), and Raman spectroscopy.

## Methodology

Fluid inclusions were studied by preparing doubly polished thin sections from a variety of ore sample types and locations in the Southeast Missouri, Tri-State, and Northern Arkansas districts. Sample locations and their corresponding identification codes are listed in Appendix I. Most of the samples in this study were collected by the principal investigator (PI) and University of Missouri—Columbia (MU) doctoral student, Zachary Wenz, whom the PI is mentoring and for whom this project constitutes a significant portion of his dissertation research. Although neither the Northern Arkansas nor the Tri-State district is actively being mined, suitable samples for study were readily found in the field. Most of the Tri-State mines are located well below the water table and are now flooded with water so that they are not easily accessible. However, many of the smaller mines have coarse tailings piles adjacent to the entrance shafts, offering sample material that is probably no more than a few tens of meters removed from its source. The topographic relief in the Northern Arkansas district is generally much greater than that in the Tri-State district and much of the mineralization occurs in shallow mines above the water table or in outcrop so that mineralization commonly could be sampled in situ. The Southeast Missouri district is still actively being mined and most of the mineralization lies in the subsurface on property of the Doe Run mining company. Samples for this study were obtained by the PI on Doe Run mine field trips and as donations from Dr. Kevin Shelton, Professor of Geological Sciences at MU, and from George Moellering, Chief Mine Geologist at Doe Run.

Doubly polished sections were prepared at low temperatures using water as a lubricant to prevent fluid inclusion stretching. In order to see clearly the abundant fluid inclusions typically present in dolomite, thin sections that consisted predominantly of dolomite were prepared to relatively

low thicknesses of 30-60 μm. Thin sections consisting predominantly of sphalerite were prepared to thicknesses of 80-120 μm. Fluid inclusion origin was based on the criteria of Goldstein and Reynolds (1994). Fluid inclusion microthermometry was performed using a Linkam™ THGMS 600 heating-cooling stage at MU. Measurement precision was ±0.1° C and estimated accuracy was ±0.2° C. Raman microprobe analysis was carried out using a JY Horiba LabRam HR800 spectrometer coupled to a LaserPhysics Reliant 100S-514 nm argon laser at the Virginia Polytechnic Institute and State University (VPI) Department of Geoscience. Elemental concentrations of inclusion fluids were measured using an Agilent 7500ce quadrupole ICP-MS coupled to a GeolasPro Excimer 193 nm ArF laser ablation at the VPI Department of Geoscience.

Reduction of the LA-ICP-MS fluid inclusion data was carried out using the ExLAM software of Zacharias and Wilkinson (2007) and the AMS 6.1.1 software of Mutchler et al. (2008). Calculation of absolute elemental concentrations in fluid inclusions was accomplished using Na as an internal standard. An independent determination of Na concentration in the fluid inclusions was obtained from the last-ice-melting temperature, which was converted to equivalent weight percent NaCl using the equation of state of Bodnar (1993). Equivalent weight percent NaCl was then converted to actual weight percent NaCl using the algorithm of Heinrich et al. (2003).

After completion of the LA-ICP-MS analyses, the paragenetic stage of the dolomite-hosted fluid inclusions from Southeast Missouri was determined by cathodoluminescence microscopy using a Nuclide Corporation cathode luminoscope in the Department of Geology and Geophysics at the Missouri University of Science and Technology.

## Results

The present study generated a total of 358 LA-ICP-MS analyses (documented in Appendix II) and hundreds of Raman microprobe analyses of fluid inclusions hosted by sphalerite, dolomite, and quartz from the Tri-State, Northern Arkansas, and Southeast Missouri districts. In addition, the study generated 374 LA-ICP-MS mineral matrix analyses of sphalerite from these three districts (Appendix III). Results are discussed below in reference to the principal objectives of the project. Additional details are presented in a manuscript by Appold and Wenz currently under review with *Economic Geology*, and in a manuscript in preparation by Wenz and Appold to be submitted to the *American Journal of Science*.

- **What was the composition of the fluids involved in MVT mineralization? In particular, what was their ore metal content?**

The elemental composition of MVT ore fluids has long been recognized to resemble that of modern sedimentary brines. However, this conclusion is based largely on bulk crush leachate analyses of MVT ore minerals that typically produce mixtures of unknown proportions of primary and secondary fluid inclusions, and are susceptible to contamination by the mineral matrix. LA-ICP-MS offers an opportunity for more rigorous characterization of MVT ore fluid

composition by analyzing individual fluid inclusions whose origin can be determined petrographically.

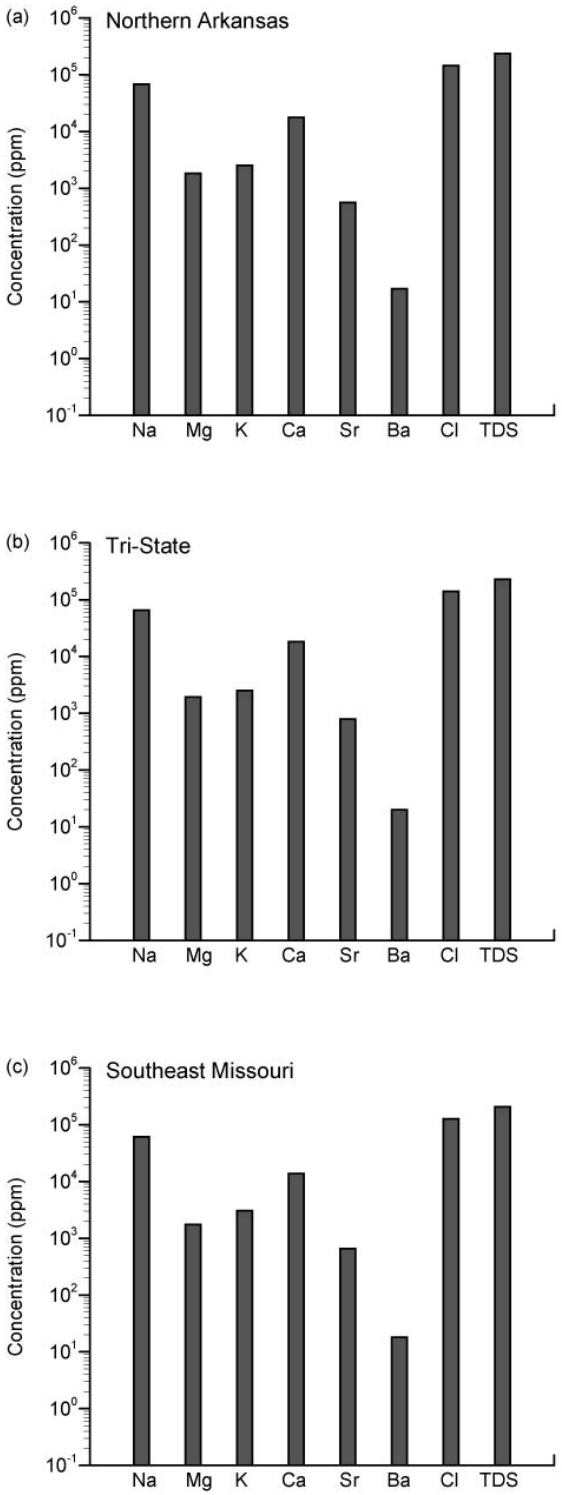


***Figure 2.*** *Major element and TDS concentrations of sphalerite-hosted fluid inclusions from the (a) Northern Arkansas, (b) Tri-State, and (c) Southeast Missouri districts.*

Figure 2 shows bar graphs of the average non-ore metal and total dissolved solids (TDS) concentrations of sphalerite-hosted fluid inclusions from the Northern Arkansas, Tri-State, and Southeast Missouri districts. The graphs show that the three districts have very similar non-ore metal compositions. Sodium is the most abundant cation in solution, followed by Ca, K, Mg, Sr, and Ba. Chloride was not measured directly but was computed by mass balance assuming that it is the only anion in solution. (In typical sedimentary brines, chloride accounts for at least 95% of the mass of anions in solution—Hanor, 1994.) Despite the overall similarities in composition, some noticeable differences exist. Southeast Missouri fluid inclusions on average are enriched in K and depleted in Ca relative to Northern Arkansas and Tri-State fluid inclusions, and Tri-State fluid inclusions are enriched in Sr relative to the other two districts.

The concentrations of the ore metals vary widely in the fluid inclusions but were highest in sphalerite-hosted fluid inclusions. Zinc could not be measured in sphalerite-hosted fluid inclusions because it is present in the sphalerite matrix in concentrations that are too high to allow the aqueous signal to be resolved in the LA-ICP-MS spectra. Lead and Cu are commonly present in significant concentrations in the sphalerite matrix. Nonetheless, Pb and to a lesser extent Cu were measurable in some fluid inclusion assemblages (FIA's). Though most fluid inclusions had Cu concentrations below the detection limit of 10's to 100's of ppm, some had very high concentrations—up to 3200 ppm in Northern Arkansas and up to 1700 ppm in Tri-State. A smaller suite of analyses from Southeast Missouri did not yield any quantifiable Cu concentrations in fluid

inclusions. As for Cu, though most fluid inclusions had Pb concentrations below the detection limit of 1's to 10's of ppm, some had very high concentrations—up to 3200 ppm in Northern Arkansas, up to 1200 ppm in Tri-State, and up to 340 ppm in Southeast Missouri. It is quite possible that higher Pb concentrations exist in some Southeast Missouri fluid inclusions, but the sphalerite from Southeast Missouri has the highest matrix Pb content of the three districts, which overwhelmed the aqueous Pb signal of many fluid inclusion analyses. This high matrix Pb content, however, argues indirectly for a high Pb concentration in the ore fluid.

- **What was the sulfur content of the mineralizing fluids?**

The concentration of ore metals and the mechanism for their precipitation is strongly dependent on the concentration and oxidation state of sulfur in the ore fluid. Thus, determination of the form and concentration of sulfur was one of the goals of the project. Sulfur is not easily quantified by LA-ICP-MS because of mass interferences with the abundant oxygen dimer. However, Raman spectroscopy is routinely used to identify sulfur species in aqueous solution and in the vapor phase of fluid inclusions.

A thorough survey of Ozark MVT fluid inclusions using Raman microprobe analysis showed $H_2S$ to be a common constituent of sphalerite-hosted fluid inclusions. The concentration of $H_2S$ in the fluid inclusions was not determined because of the experimental challenges in making synthetic $H_2S$-bearing fluid inclusions to be used as calibration standards, for which the PI does not have suitable laboratory infrastructure. Inquiries made by the PI to numerous experimental geochemists who work with $H_2S$ did not reveal any sources from which synthetic $H_2S$-bearing fluid inclusion calibration standards could be procured.

Raman microprobe analysis also showed none of the fluid inclusions hosted by any MVT mineral to contain detectable concentrations of sulfate. Because sulfate does not exist as a gas and is not toxic, synthetic fluid inclusion standards could readily be produced. The calibration standards were produced by forming solutions containing variable concentrations of $Na_2SO_4$ saturated with respect to halite at about 90° C. Upon cooling, halite crystals precipitated, trapping some of the ambient solution as fluid inclusions. Systematic Raman microprobe analysis of the fluid inclusions showed the detection limit for sulfate to be about $5\times10^{-3}$ molal (Fig. 3). Thus, Ozark MVT ore fluids can be inferred to have had sulfate concentrations less than this value.

- **What were the pH and redox potential of the mineralizing fluids?**

The pH of a fluid inclusion could in theory be determined if the concentrations of two aqueous species of an element in solution, e.g. $SO_4^{2-}$ and $HSO_4^-$ or $H_2CO_3$ and $HCO_3^-$, exist in sufficient concentrations to be quantified. No species pairs were found in sufficient concentrations to allow a pH determination to be made. However, an estimate of redox potential could be made from the concentration of methane, which Raman analysis showed to be a principal constituent of the vapor bubbles of many fluid inclusions in sphalerite, dolomite, and quartz. Redox potential estimates have so far only been made for sphalerite-hosted fluid inclusions from the Southeast Missouri district. Following the procedure of Lin et al. (2007), the partial pressure of methane in the fluid inclusion vapor bubble at room temperature could be determined from the

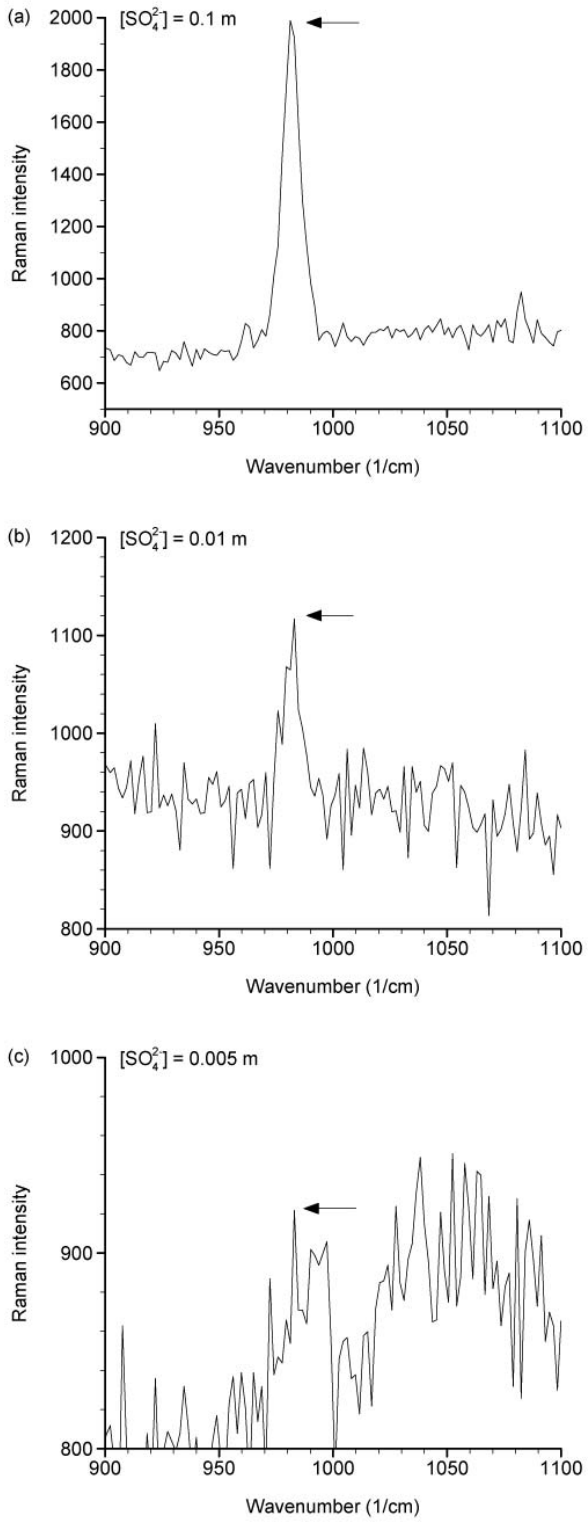


***Figure 3.*** *Raman spectra for sulfate in synthetic fluid inclusions in halite. The Raman peak for sulfate occurs at a wave number of about 983 $cm^{-1}$, indicated by the arrow, and ceases to be detectable below concentrations of about 0.005 molal.*

magnitude of the shift of the symmetric stretching band, which moves to lower wave number with increasing pressure. Assuming that all of the methane was miscible at the time of fluid inclusion entrapment, its aqueous concentration can be determined from the $H_2O$-NaCl-$CH_4$ equation of state of Duan and Mao (2006) and homogenization temperature using an iterative mass balance calculation (R. J. Bodnar, personal communication). Thus, the dissolved methane concentration of ore fluid during the time of sphalerite precipitation in Southeast Missouri appears to have been about 0.02 molal.

This methane concentration can be used to constrain the redox conditions during sphalerite precipitation. Figure 4 shows a plot of log methane solubility as a function of pH and oxygen fugacity, calculated using Geochemist's Workbench (Bethke, 2004) for an average Southeast Missouri fluid composition where total carbon content was governed by saturation with respect to dolomite. For a pH between 4 and 5, a likely range for MVT fluids (Leach & Sangster, 1993), log $f_{O_2}$ values ranging between about −54 and −55 would be predicted, causing sulfur to exist predominantly in the form of sulfide.

- **What precipitation mechanisms were most important in forming the Ozark MVT deposits?**

The fluid composition data obtained in this research has important implications for possible ore precipitation mechanisms for the Ozark MVT deposits. First, the relatively high Pb concentrations of sphalerite-hosted fluid inclusions make it unlikely, at least in the case of Tri-State and Southeast Missouri, that ore metals were transported together with sulfide in solution, as the sulfide concentration would have been

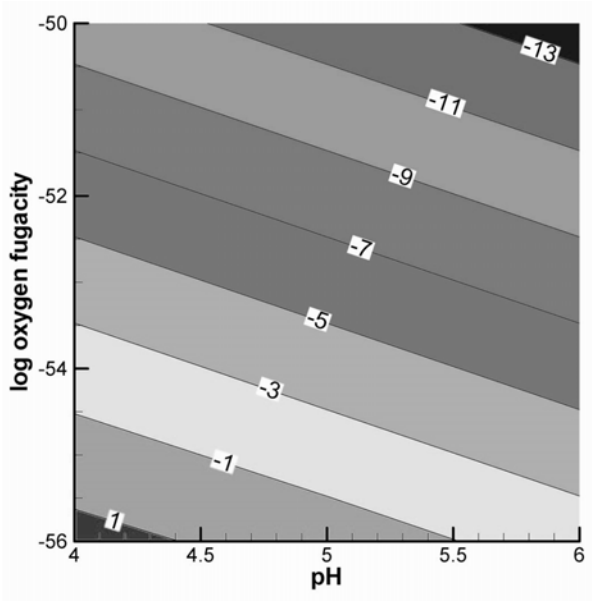


***Figure 4.*** *Contour plot of methane solubility as a function of pH and log $f_{O_2}$ for an average Southeast Missouri fluid composition where total carbon content was governed by saturation with respect to dolomite.*

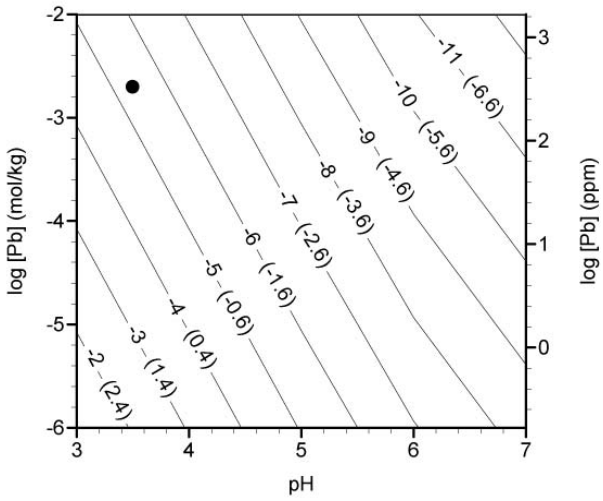


***Figure 5.*** *Contour plot of the log molal total sulfide concentration in equilibrium with galena as a function of pH and Pb concentration in a 4 molal chloride solution at 100° C and log $f_{O_2} = -60$ from Stoffell et al. (2008). The contour values shown in parentheses represent log ppm total sulfide concentrations. The dark circle near the top left corner of the plot represents the total concentration of sulfide ($4\times10^{-6}$ molal) that could coexist in solution with 340 ppm Pb (the maximum concentration measured in fluid inclusions) at a pH of 3.5 (a likely minimum for basinal brines—Hanor, 1994).*

too low to allow the observed masses of ore to have been deposited within geologically reasonable periods of time.

For example, Figure 5 shows the concentration of total sulfide in equilibrium with galena as a function of pH and Pb concentration in a 4 molal chloride solution at 100° C. The figure shows that a fluid carrying 340 ppm Pb, the maximum value found from the Southeast Missouri analyses, could only carry about $4\times10^{-6}$ molal sulfide in solution at a pH of 3.5, near the lower limit found in typical sedimentary brines (Hanor, 1994). It should be noted that the Pb concentration of the ore fluid could have been even higher than 340 ppm. The wide range of Pb concentrations in the fluid inclusions suggests some type of fluid mixing, which in the present case could have caused dilution or a pH increase of the ore fluid. Thus, the fluid inclusions would represent mixtures of varying proportions of at least two end member fluids, one of which was Pb rich and whose Pb concentration must have been at least as high as the highest concentration found in the mixture.

The low sulfide concentration able to coexist with the high Pb concentration then becomes a strong limiting factor for ore formation. Figure 6 shows a mass balance calculation representing the length of time needed to deposit all of the Viburnum Trend's $1.1\times10^{11}$ moles of sulfur bonded to the same number of moles of Pb (equivalent to about 25 million tons) in galena (Ohle and Gerdemann, 1989) as a function of aqueous sulfur concentration and Darcy velocity. As in Appold and Garven (1999), the calculation assumes a cross sectional area of flow of 10 km × 100 m, the approximate width and thickness of the St. Francois aquifer, which consists of the Lamotte Sandstone and the Bonneterre Dolomite. The most likely transport conditions are depicted by the lower gray shaded box, which could in theory extend beyond the left and bottom boundaries of the box, but would then lead to durations for ore

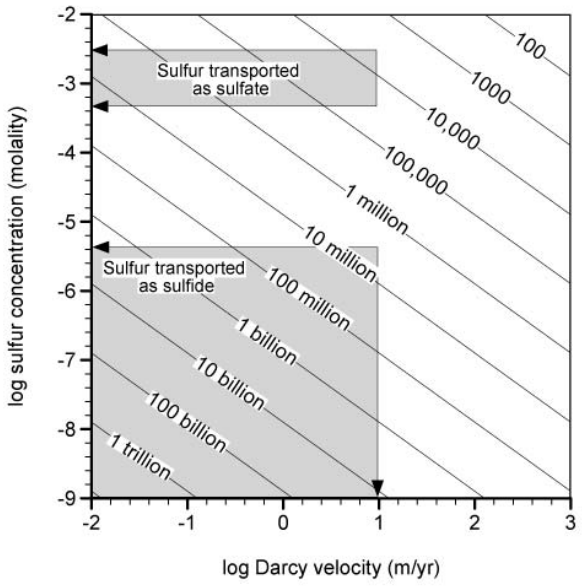


***Figure 6.*** *Mass balance calculation representing the length of time needed to deposit all of the Viburnum Trend's $1.1\times10^{11}$ moles of sulfur bonded to the same number of moles of Pb (equivalent to about 25 million tons) in galena (Ohle and Gerdemann, 1989) as a function of aqueous sulfur concentration and Darcy velocity. The calculation assumes a cross sectional area of flow of 10 km × 100 m, the approximate width and thickness of the St. Francois aquifer. If sulfur existed as sulfide, then the most likely transport conditions are depicted by the lower gray shaded box, which in theory could extend beyond the left and bottom boundaries of the plot. The right boundary of the lower box is defined by likely maximum groundwater flow rates through the St. Francois aquifer (e.g. Appold and Garven, 1999). The top boundary of the lower box is defined by the maximum sulfide concentration that is able to be transported with 340 ppm Pb at 100° C at a pH of 3.5. If sulfur existed as sulfate, then the most likely transport conditions are depicted by the upper gray shaded box, which in theory could extend beyond the left boundary of the plot. The upper and lower boundaries of the box are defined by saturation with respect to barite based on the range of Ba concentrations of 7 to 47 ppm found in the fluid inclusions. As for the lower box, the right boundary of the upper box is defined by the likely maximum groundwater flow rate through the St. Francois aquifer.*

deposition that substantially exceed the age of the Earth. The most optimal transport conditions occur at the top right corner of the lower shaded box, which corresponds to an assumed maximum Darcy velocity of about 10 m/yr (Appold and Garven, 1999) and the maximum sulfide concentration able to be transported with 340 ppm Pb at 100° C at a pH minimum of 3.5. Under these conditions, the Viburnum Trend ores could have been deposited in a still geologically reasonable time of several million years. However, for every 0.5 unit increase in pH and for every order of magnitude decrease in groundwater velocity and increase in aqueous Pb concentration, the length of time needed for ore formation increases by one order of magnitude. Thus, simultaneous transport of sulfide with Pb at concentrations of hundreds of ppm would require conditions near the limits of what is observed in nature.

It should also be noted that if sulfur was transported with Pb in the form of sulfate at concentrations of $3\times10^{-3}$ to $5\times10^{-4}$ mol/kg governed by barite saturation as noted above, then if all of the sulfate was reduced to sulfide, the Viburnum Trend's sulfur could easily have been deposited in a geological reasonable period of time, even at relatively low groundwater flow rates (see upper shaded box of Figure 6). Whether redox conditions would have allowed sulfate to exist at such concentrations is not clear. Redox conditions during sphalerite precipitation in Southeast Missouri would strongly have favored sulfide over sulfate. However, this could represent conditions caused by mixing and does not rule out the possibility that a metal-rich fluid was oxidizing with sulfur predominantly in the form of sulfate prior to mixing. Methane-rich fluid inclusions have been identified in gangue minerals from Ozark MVT deposits, suggesting that conditions were generally reducing throughout the time of MVT ore deposition. Thus, it is possible that an oxidizing, metal-rich,

sulfate-bearing fluid entered a reducing, methane-rich environment in the MVT ore districts, causing sulfate to be converted to sulfide and thus triggering the precipitation of the sulfide ore minerals. It is also possible that the metal-rich fluid was reducing and entered another reducing environment in the MVT ore districts that was enriched in $H_2S$, thus triggering sulfide ore mineral precipitation. However, the restriction of detectable $H_2S$ to sphalerite-hosted fluid inclusions suggests that sulfur entered the district with metals, and thus would favor the sulfate reduction model.

- **Did the fluids that formed giant districts like Southeast Missouri and Tri-State differ significantly in composition from those that formed small districts like Northern Arkansas?**

Fluid inclusions hosted by sphalerite offer the most direct means for comparing ore fluid chemistry among the three districts. Sphalerite in all three districts appears to have precipitated from Na-Ca-K-Mg-Cl brines with TDS concentrations between 208,000 and 235,000 ppm (Fig. 2). Fluid inclusions from Northern Arkansas on average had the highest concentrations, followed by Tri-State and Southeast Missouri. Atomic Ca/Mg ratios in sphalerite-hosted fluid inclusions average about 5.5 in all three districts (Fig. 7), which is well below the maximum of 34 needed for dolomitization (Appold & Wenz, under review). Thus, ore fluids in all three districts were relatively Mg enriched and capable of precipitating dolomite, consistent with its abundance as a gangue mineral in all three districts.

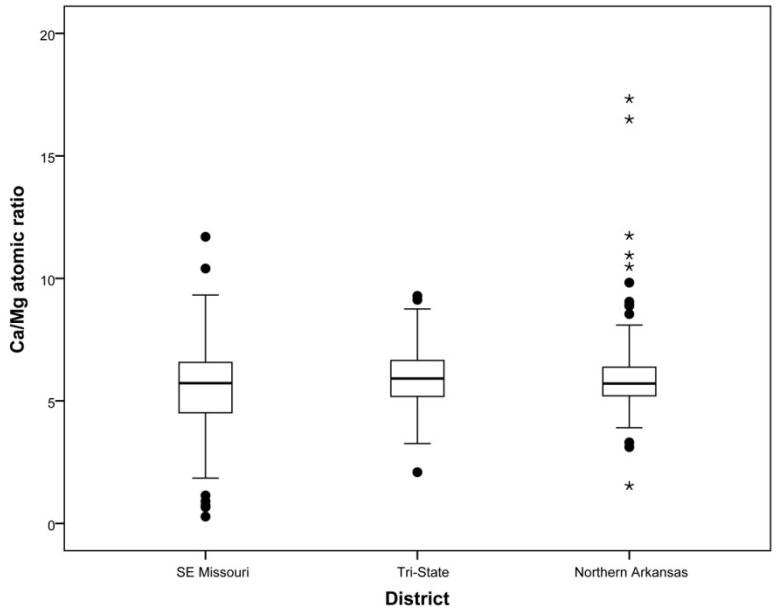


***Figure 7.*** *Box plot of atomic Ca/Mg ratios of sphalerite-hosted fluid inclusions from the Southeast Missouri, Tri-State, and Northern Arkansas districts. Here and in succeeding plots, box length represents the interquartile range, i.e. data lying between the 25th and 75th percentile. The horizontal line within each box is the median value. Data ranging within three box lengths of a box edge are plotted as outliers represented as vertical lines extending from the box. Data that are three box lengths beyond a box edge are plotted as filled circles (extreme) or stars (very extreme).*

Atomic K/Na ratios in sphalerite-hosted fluid inclusions average about 0.022 in Tri-State and Northern Arkansas and 0.028 in Southeast Missouri (Fig. 8). These values are higher by as much as an order of magnitude than those for sedimentary brines overall, but resemble the elevated K/Na ratios of more saline, deeper, and hotter sedimentary brines (Hanor, 1979; 1994; Sverjensky, 1984). This observation is consistent with hydrologic models of ore formation for the Ozark MVT deposits, in which mineralizing groundwater is shown to have penetrated deeply into the Arkoma basin below its topographic maximum, acquiring heat that it transported northward to the site of ore

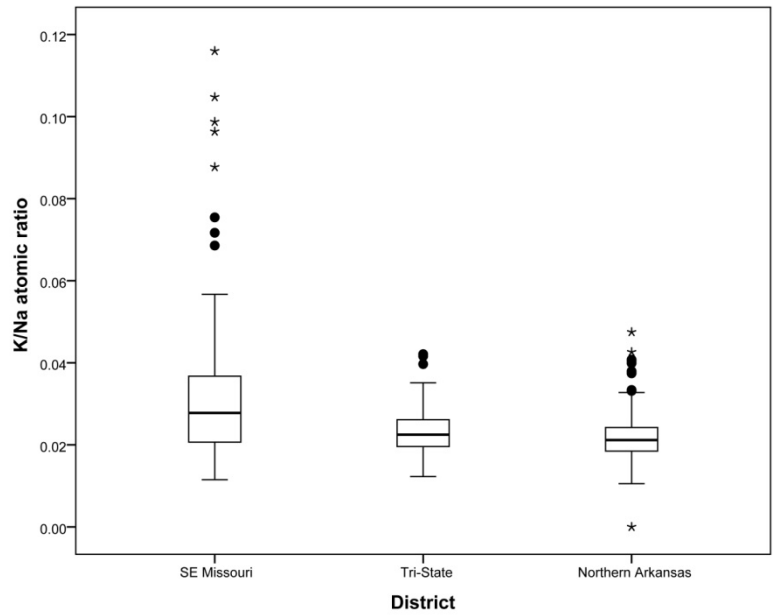


***Figure 8.*** *Box plot of atomic K/Na ratios of sphalerite-hosted fluid inclusions from the Southeast Missouri, Tri-State, and Northern Arkansas districts.*

deposition at shallower burial depths of the foreland (Garven et al., 1993; Appold and Garven, 1999; Appold & Nunn, 2005). In addition to having a higher average value, the range of Southeast Missouri K/Na ratios extends to a higher value of nearly 0.12 whereas the Tri-State and Northern Arkansas ranges reach maximum values of only 0.042 and 0.047, respectively. The high K content of Southeast Missouri ore fluid was likely acquired through interaction with granitic basement rock and the basal arkosic section of the Cambrian Lamotte Sandstone at shallower depths closer to or within the Southeast Missouri district (Lentini and Shanks, 1983; Rothbard, 1983; Diehl and Goldhaber, 1995). The Tri-State and Northern Arkansas ores are hosted by younger Ordovician and Mississippian carbonates and are not as close to K rich source rocks.

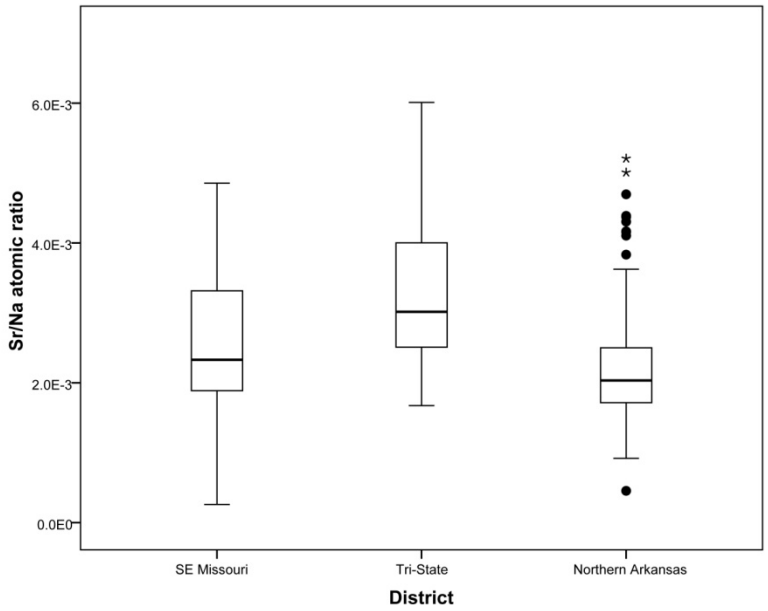


***Figure 9.*** *Box plot of atomic Sr/Na ratios of sphalerite-hosted fluid inclusions from the Southeast Missouri, Tri-State, and Northern Arkansas districts.*

Atomic Sr/Na ratios in sphalerite-hosted fluid inclusions average about $2.0\times10^{-3}$ in Northern Arkansas, $2.4\times10^{-3}$ in Southeast Missouri, and $3.0\times10^{-3}$ in Tri-State (Fig. 9). These values are typical of sedimentary brines. The reason for these differences is not clear, and the differences are also not very large, but they may reflect differences in the degree of alteration (dolomitization and silicification) of the host limestone, which would have released Sr into solution, and in the original Sr content of the host limestone.

Sphalerite-hosted fluid inclusions from Northern Arkansas have

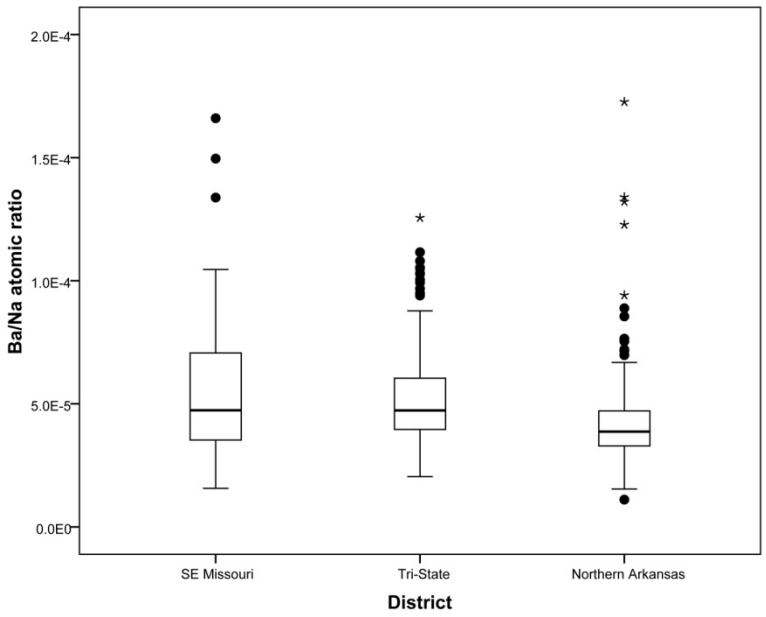


***Figure 10.*** *Box plot of atomic Ba/Na ratios of sphalerite-hosted fluid inclusions from the Southeast Missouri, Tri-State, and Northern Arkansas districts.*

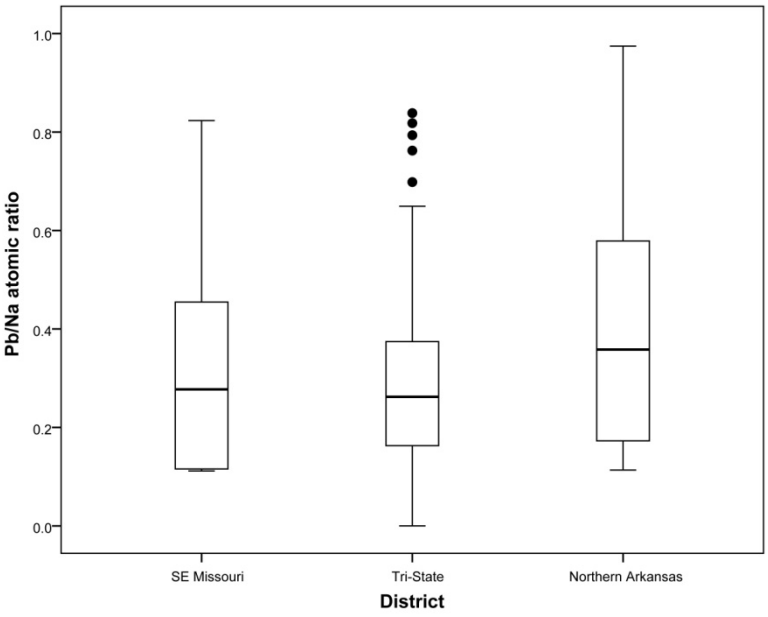


***Figure 11.*** *Box plot of atomic Pb/Na ratios of sphalerite-hosted fluid inclusions from the Southeast Missouri, Tri-State, and Northern Arkansas districts.*

average atomic Ba/Na ratios of about $4.0\times10^{-5}$ that are slightly lower than the average ratio of $5.0\times10^{-5}$ in Southeast Missouri and Tri-State (Fig. 10). In contrast, atomic Pb/Na ratios in Northern Arkansas are slightly higher at about $4.0\times10^{-4}$ instead of about $2.8\times10^{-4}$ in Southeast Missouri and Tri-State (Fig. 11). The differences among the districts are not very large, though the Northern Arkansas data set has a few very Pb rich outliers at values of around 2100 ppm that suggest the presence of a particularly Pb rich end member fluid in the district.

## Summary and Conclusions

The results of this study have confirmed that MVT deposits in the Southeast Missouri, Tri-State, and Northern Arkansas districts precipitated from fluids that resemble typical deep sedimentary basinal brines. The overall compositions of fluid inclusions in the three districts are similar to one another, with TDS concentrations between 208,000 and 235,000 ppm consisting principally of the cations Na, Ca, K, Mg, Sr, and Ba ranked in decreasing order of abundance, with Cl presumed to be the principal anion. Subtle compositional variations existed among ore fluids of the districts, as evidenced by fluid inclusions hosted by sphalerite. Fluid inclusions from Southeast Missouri are enriched in potassium relative to Tri-State and Northern Arkansas. Northern Arkansas fluid inclusions have the lowest Sr/Na and Ba/Na ratios and the highest Pb/Na ratios

and average TDS concentration of the three districts. The potassium enrichment in Southeast Missouri is most likely related to the ores' proximity to granitic basement rocks. Northern Arkansas and Tri-State ores are located in stratigraphically higher rocks that are not near any potassium rich source rocks. The reasons for the other geochemical differences are currently not clear, but a correlation between Pb concentration and salinity is consistent with the greater solubility of Pb in higher salinity fluids because of the effects of chloride complexing. Why the highest Pb aqueous concentrations should be in the smallest of the three districts could be because the least metal was precipitated from the fluid, perhaps because of a lower supply of sulfide or reductant at the site of ore deposition.

Though Pb concentrations were highest in fluid inclusions from the Northern Arkansas district, each of the districts had a population of Pb rich fluid inclusions with concentrations on the order of at least 100's of ppm in Southeast Missouri and 1000's of ppm in Tri-State and Northern Arkansas. Careful examination of the LA-ICP-MS spectra of these analyses shows that the Pb signals from which the concentrations were computed are in fact consistently associated with the aqueous phase and are unlikely to represent Pb rich mineral inclusions or solid solution. Cu was a more difficult element to quantify and was not successfully detected in Southeast Missouri fluid inclusions. However, some sphalerite-hosted fluid inclusions from Tri-State and Northern Arkansas had Cu concentrations on the order of 1000's of ppm. The Pb and Cu rich fluid inclusions appear to be limited to sphalerite and were not found in any of the gangue mineral hosts. These observations lead to the conclusion that ore deposition in each of the three MVT districts involved invasion of a metal rich brine. The low sulfide concentration that could be carried with these high metal concentrations makes it unlikely that metals and sulfide were transported together in the same solution. Instead, metals were most likely transported either with sulfate in an oxidizing fluid where sulfide mineral deposition was induced by mixing with some kind of a reductant, or in a sulfur poor fluid where sulfide mineral deposition was induced by mixing with a $H_2S$ rich fluid.

To distinguish between these two possibilities, fluid inclusions were analyzed by Raman spectroscopy to try to identify any sulfur species present. Sulfate was not detected in any fluid inclusions analyzed, though its detection limit was relatively high at around $5\times10^{-3}$ molal. $H_2S$ was detected in many sphalerite-hosted fluid inclusions but not in any gangue mineral-hosted fluid inclusions. Though the concentration of $H_2S$ could not be quantified, its prevalence suggests reducing conditions during the time of sulfide mineral precipitation. This conclusion is supported by the coexistence of abundant methane in sphalerite-hosted fluid inclusions from Southeast Missouri, from which a likely $\log f_{O_2}$ value between −54 and −55 could be calculated. That $H_2S$ was present and conditions were reducing during the time of sphalerite precipitation does not indicate whether a metal rich fluid mixed with a $H_2S$ rich fluid or whether sulfate in a metal rich fluid was reduced to sulfide by methane or another reductant at the site of ore deposition, as both processes would have resulted in reducing, $H_2S$ rich conditions. However, the fact that methane was present throughout the paragenesis but $H_2S$ only during the time of sphalerite deposition suggests that conditions were generally reducing in the ore districts and sulfur was introduced with metals during times of sphalerite precipitation. This would favor a sulfate reduction model for ore deposition.

## References


Appold, M. S., and Garven, G., 1999, The hydrology of ore formation in the southeast Missouri district: numerical models of topography-driven fluid flow during the Ouachita orogeny: Economic Geology, v. 94, p. 913-936.

Appold, M. S. and Nunn, J. A., 2005, Hydrology of the western Arkoma basin and Ozark platform during the Ouachita orogeny: implications for Mississippi Valley-type ore formation in the Tri-State Zn-Pb district: Geofluids, v. 5, p. 308-325.

Bethke, C. M., 2004, The Geochemist's Workbench® Release 5: GWB Reference Manual: Urbana, Illinois, University of Illinois, 225 p.

Bodnar, R. J., 1993, Revised equation and table for determining the freezing point depression of $H_2O$-NaCl solutions: Geochimica et Cosmochimica Acta, v. 57, p. 683-684.

Diehl, S. F., and Goldhaber, M. B., 1995, Feldspar diagenesis in Cambrian clastic rocks of the southern Ozark Mountains and Reelfoot rift, southeastern Missouri and northeastern Arkansas—implications for Mississippi Valley-type ore genesis: U.S. Geological Survey Bulletin 1989, F1-F17.

Duan, Z, Mao, S., 2006, A thermodynamic model for calculating methane solubility, density and gas phase composition of methane-bearing aqueous fluids from 273 to 523 K and from 1 to 2000 bar: Geochimica et Cosmochimica Acta, v. 70, p. 3369-3386.

Garven, G., Ge, S., Person, M. A. and Sverjensky, D. A., 1993, Genesis of stratabound ore deposits in the mid-continent basins of North America. 1. The role of regional groundwater flow: American Journal of Science, v.293, p.497-568.

Goldstein, R. H., and Reynolds, T. J., 1994, Systematics of fluid inclusions in diagenetic minerals: Society of Economic Geologists and Paleontologists Short Course 31, 199 p.

Hanor, J. S., 1979, The sedimentary genesis of hydrothermal fluids, *in*, Barnes, H. L., ed., Geochemistry of Hydrothermal Ore Deposits: New York, Wiley, p. 137-172.

Hanor, J. S., 1994, Origin of saline fluids in sedimentary basins, *in*, Parnell, J., ed., Geofluids: Origin, Migration and Evolution of Fluids in Sedimentary Basins: Geological Society Special Publication No. 78, p. 151-174.

Heinrich, C. A., Pettke, T., Halter, W. E., Aigner-Torres, M., Audetat, A., Günther, D., Hattendorf, B., Bleiner, D., Guillong, M., and Horn, I., 2003, Quantitative multi-element analysis of minerals, fluid and melt inclusions by laser-ablation inductively-coupled-plasma mass-spectrometry: Geochimica et Cosmochimica Acta, v. 67, p. 3473-3496.

Leach, D. L., Sangster, D. F., 1993, Mississippi Valley-type Lead-Zinc Deposits, *in*, Kirkham, R. V., Sinclair, W. D., Thorpe, R. I., and Duke, J. M., eds., Mineral Deposit Modeling: Geological Association of Canada Special Paper 40, p. 289-314.

Lentini, M. R., and Shanks III, W. C., 1983, Experimental study of brine-arkose interaction at 200°C and 500 bars: origin of metalliferous oil field brines and Mississippi Valley-type ore deposits, *in*, Kisvarsanyi, G., Grant, S. K., Pratt, W. P., and Koenig, J. W., eds., International Conference on Mississippi Valley-type Lead-Zinc Deposits: Rolla, Missouri, University of Missouri—Rolla, p. 195-205.

Lin, F., Bodnar, R. J., Becker, S. P., 2007, Experimental determination of the Raman $CH_4$ symmetric stretching ($\nu_1$) band position from 1-650 bar and 0.3-22 °C: Application to fluid inclusion studies: Geochimica et Cosmochimica Acta, v. 71, p. 3746-3756.

Mutchler, S. R., Fedele, L., and Bodnar, R. J., 2008, Appendix A5: Analysis management system (AMS) for reduction of laser ablation ICP-MS data, *in*, Sylvester, P., ed., Laser Ablation ICP–MS in the Earth Sciences: Current Practices and Outstanding Issues: Vancouver, Mineralogical Association of Canada Short Course 40, p. 318-327.

Ohle, E. L., and Gerdemann, P. E., 1989, Recent exploration history in southeast Missouri: Society of Economic Geologists Guidebook Series, v. 5, p. 1-11.

Rothbard, D. R., 1983, Diagenetic history of the Lamotte Sandstone, southeast Missouri, *in*, Kisvarsanyi, G., Grant, S. K., Pratt, W. P., and Koenig, J. W., eds., International Conference on Mississippi Valley-type Lead-Zinc Deposits: Rolla, Missouri, University of Missouri—Rolla, p. 385-395.

Sverjensky, D. A., 1984, Oil field brines as ore-forming solutions: Economic Geology, v. 79, p. 23-37.

Sverjensky, D. A., 1986, Genesis of Mississippi Valley-type zinc-lead deposits: Annual Review of Earth and Planetary Sciences, v. 14, p. 177-199.

Zacharias, J., and Wilkinson, J., 2007, ExLAM 2000: Excel VBA application for processing of transient signals from laser ablation (LA-ICP-MS) of fluid inclusions and solid phases [abstr.]: ECROFI-XIX Biennial Conference on European Current Research on Fluid Inclusions, Bern, Switzerland.

## Publications Resulting from Grant

**Conference Abstracts:**

Appold, M. S., Wenz, Z. J., 2009, Implications of Pb-rich fluid inclusions from Mississippi Valley-type ore deposits of the Viburnum Trend, Southeast Missouri: Geological Society of America, Abstracts with Programs, v. 41, 93-3.

Wenz, Z. J., Appold, M. S., 2009, Chemical variation of inclusion fluids in Ozark MVT deposits determined by LA-ICP-MS: implications for deposit size and ore precipitation mechanisms: American Geophysical Union, Toronto, ON, May 25, 2009.

**Manuscripts under Review:**

Appold, M. S., Wenz, Z. J. (submitted August 4, 2009) Composition of ore fluid inclusions from the Viburnum Trend, Southeast Missouri district, USA: implications for transport and precipitation mechanisms: Economic Geology.

**Manuscripts in Preparation:**

Wenz, Z. J., Appold, M. S. (in preparation) Regional synthesis of the geochemistry of Mississippi Valley-type ore-forming fluids in the Ozark Plateau: American Journal of Science.

**Doctoral Dissertation in Preparation:**

Wenz, Z. J. (in preparation) Fluid geochemistry and origin of Mississippi Valley-type mineralization in the Ozark Plateau: University of Missouri—Columbia.

# Appendix I

## Sample Locations

| Sample ID | Latitude (°N) | Longitude (°W) | Location Description |
|---|---|---|---|
| ***Northern Arkansas district*** | | | |
| NACP | 36.34052 | 92.80845 | Copper Head mine |
| NAEX | 36.04055 | 92.82385 | Excelsior mine |
| NAJP | 36.30061 | 92.90611 | Jackpot mine |
| NALB | 36.33995 | 92.65308 | Lost Belle mine |
| NALD | 36.06567 | 92.74422 | Lucky Dog mine |
| NAMC | 36.13052 | 92.55152 | Monte Cristo mine |
| NAPA | 36.13290 | 92.54938 | Philadelphia mine |
| | | | |
| ***Southeast Missouri district*** | | | |
| 35_8V22 | 37.65972 | 91.12667 | Casteel mine |
| 81V22 | 37.65972 | 91.12667 | Casteel mine |
| MAG13 | 37.63944 | 91.12250 | Magmont mine |
| MAG13A | 37.63944 | 91.12250 | Magmont mine |
| VTSW2 | 37.35972 | 91.14583 | Sweetwater mine |
| VTSW2E | 37.35972 | 91.14583 | Sweetwater mine |
| VTSW2F | 37.35972 | 91.14583 | Sweetwater mine |
| WF | 37.49167 | 91.10833 | West Fork mine |
| WF2B | 37.49167 | 91.10833 | West Fork mine |
| | | | |
| ***Tri-State Missouri district*** | | | |
| TSBS3 | 37.03271 | 94.75474 | Baxter Springs, KS |
| TSBS5 | 37.24322 | 94.42198 | Baxter Springs, KS |
| TSCM2 | 37.01602 | 94.85260 | Commerce, OK |
| TSDW2 | 37.11122 | 94.41595 | Duenweg, MO |
| TSGY2 | 36.91210 | 94.24985 | Granby, MO |
| TSNC1 | 37.25052 | 94.44488 | Neck City, MO |
| TSPC2 | 36.96418 | 94.81046 | Picher, OK |
| TSPC7 | 36.97038 | 94.85997 | Picher, OK |
| TSTR1 | 37.01602 | 94.85260 | Treece, KS |
| TSWB3 | 37.01468 | 94.86025 | Treece, KS |
| TSWC1 | 37.15292 | 94.45368 | Webb City, MO |

# Appendix II

## LA-ICP-MS Elemental Composition Analyses of Fluid Inclusions from Ozark MVT Deposits

| Sample ID | Mineral Host | Fluid inclusion # | Th1 | Th2 | Tm1 | Tm2 | Na ppm | Mg ppm | K ppm | Ca ppm | Cu ppm | Sr ppm | Ba ppm | Pb ppm |
|---|---|---|---|---|---|---|---|---|---|---|---|---|---|---|
| ***Northern Arkansas district*** | | | | | | | | | | | | | | |
| NAMC1-4 | dolomite | 1 | 141 | 142 | -22.8 | -22.7 | 92479 | | 3495 | | | 1225 | 17 | |
| NAMC1-4 | dolomite | 1 | 137 | 138 | -22.3 | -22.4 | 89548 | | 4298 | | | | 22 | |
| NAMC1-4 | dolomite | 3 | 136 | 137 | -22.3 | -22.4 | 91034 | | 2593 | | | 576 | 14 | |
| NAEX1-7 | dolomite | 2 | 126 | 127 | -21 | -21.1 | 87842 | | 3618 | | | 602 | 14 | |
| NAEX1-7 | dolomite | 3 | 127 | 128 | -19.7 | -19.8 | 82533 | | 6258 | | | 649 | 25 | |
| NAEX1-7 | dolomite | 6 | 126 | 127 | -21 | -21.1 | 86618 | | | | | | 13 | |
| NAJP1-1 | dolomite | 1 | 132 | 133 | -21.3 | -21.4 | 88832 | | 3570 | | | 943 | 36 | |
| NAJP1-1 | dolomite | 1 | 116 | 117 | -20.8 | -20.7 | 86991 | | 3930 | | | 1123 | 22 | |
| NALD1-1 | dolomite | 1 | 132 | 133 | -11.8 | -11.9 | 60388 | | 2017 | | | 791 | 6 | 1 |
| NALD1-1 | dolomite | 1 | 118 | 119 | -11.7 | -11.8 | 59468 | | 3129 | | | 787 | 16 | |
| NALD1-1 | dolomite | 1 | 136 | 137 | -18.5 | -18.6 | 81109 | | 3885 | | | 1356 | 9 | |
| NAPA1-1 | dolomite | 1 | 118 | 119 | -18.7 | -18.6 | 81291 | | 3669 | | | 633 | 13 | |
| NAPA1-1 | dolomite | 2 | 136 | 137 | -23.1 | -23.2 | 91352 | | 4256 | | | | 53 | |
| NAPA1-1 | dolomite | 4 | 135 | 136 | -23.3 | -23.4 | 95002 | | | | | | | |
| NAPA1-1 | dolomite | 6 | 115 | 116 | -22.8 | -22.7 | 92767 | | 2628 | | | 776 | 11 | |
| NAPA1-1 | dolomite | 7 | 142 | 143 | -23 | -23.1 | 93164 | | 3231 | | | 726 | 19 | |
| NAPA1-1 | dolomite | 8 | 146 | 147 | -23 | -23.1 | 92971 | | 3672 | | | 949 | 14 | |
| NAPA1-1 | dolomite | 9 | 137 | 138 | -22.7 | -22.8 | 93035 | | | | | | 24 | |
| NAPA1-1 | dolomite | 10 | 133 | 134 | -22.7 | -22.8 | 92739 | | | | | | 38 | |
| NAPA1-1 | dolomite | 11 | 122 | 123 | -17.7 | -17.6 | 78353 | | 3653 | | | 764 | | 36 |
| NAMC1-4 | dolomite | 1 | 141 | 142 | -22.8 | -22.7 | 92479 | | 3495 | | | 1225 | 17 | |
| NAPA1-13 | quartz | 5 | 110 | | -22 | -21.9 | 72057 | 956 | 1550 | 16306 | | 493 | 10 | |
| NAPA1-13 | quartz | 7 | 105 | 106 | -22 | -21.9 | 70497 | 963 | 2902 | 17003 | | 598 | 29 | |
| NACP1-8 | sphalerite | 1 | 109 | 110 | -20.4 | -20.3 | 66457 | 1577 | 2184 | 16570 | | 578 | 17 | |
| NACP1-8 | sphalerite | 1 | 102 | 103 | -22.5 | -22.4 | 62498 | 1876 | 1927 | 24951 | | 546 | 17 | |
| NACP1-8 | sphalerite | 2 | 98 | 99 | -22.7 | -22.6 | 72216 | 1670 | 2027 | 16698 | | 533 | 16 | |
| NACP1-8 | sphalerite | 1 | 108 | 109 | -23.2 | -23.1 | 69090 | 1828 | 2650 | 20003 | | 648 | 17 | |
| NACP1-8 | sphalerite | 2 | 100 | 101 | -23.3 | -23.4 | 66517 | 2444 | 3328 | 21099 | | 724 | 26 | |
| NAPA1-13B | sphalerite | 2 | 90 | 91 | -21.6 | -21.5 | 66189 | 1683 | 3732 | 18633 | | 397 | 10 | |
| NAPA1-13B | sphalerite | 3 | 80 | 81 | -21.9 | -21.8 | 71156 | 1459 | 2623 | 15800 | | 481 | 10 | |
| NALD1-2 | sphalerite | 1 | 113 | 114 | -20.1 | -20 | 66839 | 1732 | 5398 | 13012 | | 270 | 8 | |
| NALD1-2 | sphalerite | 1 | 105 | 106 | -19.5 | -19.4 | 64523 | 1769 | 2905 | 15561 | | 334 | 12 | 34 |
| NAPA1-13 | sphalerite | 1 | 101 | 102 | -21 | -21.1 | 66467 | 2083 | 2699 | 17348 | | 382 | 19 | |
| NAPA1-13 | sphalerite | 2 | 100 | 101 | -21.5 | -21.4 | 66630 | 1861 | 2732 | 18423 | | 405 | 13 | |
| NAPA1-13 | sphalerite | 3 | 139 | 140 | -21 | -20.9 | 59817 | 2550 | 1899 | 22993 | | 554 | 17 | |
| NACP1-8 | sphalerite | 1 | 115 | 116 | -22 | -22.1 | 59050 | 2199 | | 26508 | | 1127 | 14 | |
| NAJP1-3 | sphalerite | 1 | 99 | 100 | -22.5 | -22.4 | 67898 | 2606 | 2430 | 18110 | 230 | 524 | 19 | 643 |
| NAJP1-3 | sphalerite | 2 | 100 | 101 | -22.5 | -22.4 | 70959 | 1900 | 2484 | 16648 | 75 | 535 | 15 | 17 |
| NAJP1-3o | sphalerite | 1 | 100 | 101 | -23 | -22.9 | 66006 | 2510 | 4203 | 20373 | | 606 | 13 | |
| NAMC1-1 | sphalerite | 1 | 136 | 137 | -23 | -22.9 | 69483 | 1810 | | 20091 | | 574 | 24 | |
| NAMC1-1 | sphalerite | 2 | 138 | 139 | -23 | -22.9 | 70368 | 1806 | 1541 | 19251 | | 554 | 27 | |

| Sample ID | Mineral Host | Fluid inclusion # | Th1 | Th2 | Tm1 | Tm2 | Na ppm | Mg ppm | K ppm | Ca ppm | Cu ppm | Sr ppm | Ba ppm | Pb ppm |
|---|---|---|---|---|---|---|---|---|---|---|---|---|---|---|
| NAMC1-1 | sphalerite | 3 | 133 | 134 | -23 | -22.9 | 68716 | 2433 | 1430 | 19876 | | 674 | 31 | |
| NAMC1-1 | sphalerite | 1 | 110 | 111 | -23.1 | -23.2 | 70829 | 1856 | 2411 | 18589 | | 558 | 17 | |
| NAMC1-1 | sphalerite | 2 | 110 | 111 | -23.1 | -23.2 | 74006 | 583 | 3336 | 16646 | | 393 | 18 | |
| NAEX1-7 | sphalerite | 2 | 129 | 130 | -21 | -21.1 | 52900 | 1494 | 3667 | 21875 | | 882 | 55 | |
| NAEX1-7 | sphalerite | 1 | 115 | 116 | -16 | -16.1 | 51517 | 1434 | 2644 | 14151 | | 845 | 11 | 103 |
| NAEX1-7 | sphalerite | 2 | 113 | 114 | -16 | -16.1 | 53236 | 1706 | 2193 | 17001 | | 1057 | 9 | |
| NAEX1-7 | sphalerite | 3 | 113 | 114 | -16 | -16.1 | 53561 | 1202 | 3635 | 15534 | | 959 | 24 | 1949 |
| NAEX1-7 | sphalerite | 4 | 113 | 114 | -16 | -16.1 | 52719 | 2067 | 2004 | 16833 | | 825 | 11 | 853 |
| NAEX1-7 | sphalerite | 1 | 113 | 114 | -20.3 | -20.4 | 66860 | 1608 | 2068 | 16317 | | 535 | 15 | 83 |
| NAEX1-7 | sphalerite | 2 | 113 | 114 | -20.5 | -20.6 | 66443 | 1700 | 1477 | 17527 | | 434 | 10 | |
| NACP1-8 | sphalerite | 2 | 96 | 97 | -22.1 | -22.2 | 67583 | 2116 | 2155 | 19053 | | 649 | 19 | |
| NACP1-8 | sphalerite | 2 | 86 | 87 | -21.5 | -21.6 | 66222 | 1481 | 2385 | 19654 | | 638 | 17 | |
| NAEX1-14 | sphalerite | 1 | 109 | 110 | -21.9 | -22 | 66775 | 2374 | 4589 | 17380 | | 516 | 16 | |
| NAEX1-14 | sphalerite | 2 | 110 | 111 | -22.2 | -22.1 | 72091 | 1638 | 2244 | 15632 | | 496 | 15 | |
| NAEX1-2 | sphalerite | 1 | 101 | 102 | -22.9 | -22.8 | 70647 | 1841 | 2394 | 18129 | | 561 | 18 | |
| NAEX1-2 | sphalerite | 2 | 100 | 101 | -22.9 | -22.8 | 72204 | 1644 | 1905 | 17281 | | 610 | 22 | |
| NAEX1-2 | sphalerite | 3 | 100 | 101 | -22.9 | -22.8 | 72039 | | | 18187 | | 613 | 21 | |
| NAJP1-10 | sphalerite | 1 | 103 | 104 | -22.7 | -22.8 | 69036 | 2053 | 1961 | 18065 | 696 | 562 | 19 | 47 |
| NAJP1-10 | sphalerite | 2 | 101 | 102 | -22.6 | -22.7 | 68467 | 2584 | 2320 | 18635 | 1948 | 621 | 20 | 283 |
| NAJP1-10 | sphalerite | 3 | 102 | 103 | -22.6 | -22.7 | 66272 | 2120 | 2052 | 18407 | 2846 | 705 | 20 | |
| NAJP1-10 | sphalerite | 4 | 102 | 103 | -22.7 | -22.8 | 68756 | 2018 | 1992 | 18595 | 435 | 479 | 14 | 95 |
| NALB1-1 | sphalerite | 1 | 88 | 89 | -22.8 | -22.9 | 68570 | 2169 | 2155 | 19658 | | 653 | 16 | 29 |
| NALB1-1 | sphalerite | 2 | 88 | 89 | -22.8 | -22.9 | 68380 | 2456 | | 16796 | 1671 | 510 | 12 | 3211 |
| NALB1-1 | sphalerite | 1 | 107 | 106 | -21.9 | -22 | 69839 | 1900 | 2035 | 16974 | | 549 | 17 | |
| NALB1-1 | sphalerite | 2 | 107 | 108 | -22 | -22.1 | 69147 | 2262 | 2193 | 17206 | | 567 | 21 | |
| NALD1-4 | sphalerite | 4 | 115 | 116 | -22.7 | -22.8 | 67564 | 1467 | 3023 | 20668 | | 775 | 53 | |
| NAMC1-1 | sphalerite | 1 | 99 | 100 | -22.2 | -22.3 | 69720 | 1950 | 2478 | 17395 | | 559 | 18 | |
| NAMC1-1 | sphalerite | 2 | 102 | 103 | -22.2 | -22.3 | 70919 | 1515 | 2503 | 16854 | | 615 | 18 | |
| NAMC1-1 | sphalerite | 3 | 102 | 103 | -22.2 | -22.3 | 68275 | 1972 | 1863 | 19141 | | 514 | 23 | |
| NAMC1-1 | sphalerite | 4 | 102 | 103 | -22.2 | -22.3 | 70015 | 1977 | 2526 | 17039 | | 579 | 19 | |
| NAMC1-1 | sphalerite | 5 | 103 | 104 | -22.2 | -22.3 | 70184 | 1416 | 2660 | 17609 | | 544 | 16 | |
| NAMC1-1 | sphalerite | 6 | 103 | 104 | -22.2 | -22.3 | 70677 | 1753 | 1687 | 17355 | | 532 | 20 | |
| NAMC1-1 | sphalerite | 1 | 106 | 107 | -22.1 | -22.2 | 70806 | 1694 | 2183 | 16765 | | 511 | 16 | |
| NAMC1-1 | sphalerite | 2 | 99 | 100 | -22.1 | -22.2 | 71436 | 1797 | 2201 | 16004 | | 547 | 14 | |
| NAMC1-1 | sphalerite | 1 | 129 | 130 | -22.2 | -22.3 | 71253 | 1706 | 2696 | 15298 | 1128 | 473 | 16 | 164 |
| NAMC1-1 | sphalerite | 2 | 133 | 134 | -22.2 | -22.3 | 74764 | 1726 | | 14824 | | 502 | 18 | |
| NAMC1-1 | sphalerite | 4 | 129 | 130 | -22.2 | -22.3 | 71250 | 1494 | 2481 | 16668 | | 506 | 17 | |
| NAMC1-1 | sphalerite | 2 | 124 | 125 | -22.2 | -22.3 | 72587 | 1741 | 1740 | 15614 | | 485 | 17 | |
| NAMC1-1 | sphalerite | 3 | 128 | 129 | -22.2 | -22.3 | 70868 | 1345 | 3342 | 16627 | | 522 | 15 | |
| NAMC1-1 | sphalerite | 4 | 128 | 129 | -22.2 | -22.3 | 72254 | 1974 | | 16131 | | 505 | 10 | |
| NAMC1-1 | sphalerite | 2 | 105 | 106 | -22.3 | -22.4 | 69188 | 2076 | 2240 | 18129 | | 519 | 12 | |
| NAMC1-1 | sphalerite | 3 | 105 | 106 | -22.3 | -22.4 | 73186 | 1200 | 2365 | 15639 | 3198 | 471 | 18 | 236 |
| NAMC1-1 | sphalerite | 4 | 105 | 106 | -22.3 | -22.4 | 72216 | 1706 | 2065 | 15984 | 675 | 529 | 15 | 82 |
| NAMC1-1 | sphalerite | 5 | 105 | 106 | -22.3 | -22.4 | 71960 | 1733 | 1448 | 16630 | | 491 | 15 | |
| NAMC1-1 | sphalerite | 6 | 105 | 106 | -22.3 | -22.4 | 69822 | 2083 | 2307 | 17475 | | 540 | 16 | |
| NAMC1-1 | sphalerite | 8 | 105 | 106 | -22.3 | -22.4 | 69822 | 2083 | 2307 | 17475 | | 540 | 16 | |
| NAPA1-13 | sphalerite | 1 | 101 | 102 | -21.1 | -21.2 | 69480 | 1622 | 2665 | 15513 | | 357 | 14 | |

| Sample ID | Mineral Host | Fluid inclusion # | Th1 | Th2 | Tm1 | Tm2 | Na ppm | Mg ppm | K ppm | Ca ppm | Cu ppm | Sr ppm | Ba ppm | Pb ppm |
|---|---|---|---|---|---|---|---|---|---|---|---|---|---|---|
| NAPA1-13 | sphalerite | 2 | 101 | 102 | -21.1 | -21.2 | 62493 | 2530 | 3482 | 19884 | | 646 | 26 | |
| NAPA1-13 | sphalerite | 5 | 101 | 102 | -21.1 | -21.2 | 69969 | 1490 | 2632 | 15275 | | 357 | 11 | |
| NAPA1-13 | sphalerite | 6 | 101 | 102 | -21.1 | -21.2 | 67913 | 1798 | 2381 | 16861 | | 416 | 13 | |
| NAPA1-13 | sphalerite | 7 | 102 | 103 | -21.1 | -21.2 | 69659 | 1614 | 2852 | 15224 | | 368 | 14 | |
| NAPA1-13 | sphalerite | 8 | 101 | 102 | -21.1 | -21.2 | | | | | | | | |
| NAMC1-1 | sphalerite | 1 | 103 | 104 | -22.3 | -22.4 | 73212 | 1744 | 2387 | 14839 | | 456 | 19 | |
| NAMC1-1 | sphalerite | 3 | 103 | 104 | -22.3 | -22.4 | 74659 | 1335 | 1439 | 14748 | | 447 | 19 | |
| NAMC1-1 | sphalerite | 4 | 103 | 104 | -22.3 | -22.4 | 70888 | 2038 | 2399 | 16523 | | 497 | 17 | |
| NAMC1-1 | sphalerite | 6 | 107 | 108 | -22.3 | -22.4 | 71190 | 1505 | 1717 | 17444 | | 539 | 14 | |
| NAMC1-1 | sphalerite | 7 | 108 | 109 | -22.3 | -22.4 | 71988 | 1703 | 2392 | 15990 | | 503 | 14 | |
| NAMC1-1 | sphalerite | 8 | 107 | 108 | -22.3 | -22.4 | 72871 | 1728 | 2010 | 15384 | | 530 | 24 | |
| NAPA1-13 | sphalerite | 1 | 94 | 95 | -21 | -20.9 | 70239 | 1537 | 2604 | 14490 | 334 | 379 | 13 | 52 |
| NAPA1-13 | sphalerite | 2 | 100 | 101 | -21 | -21.1 | 69183 | 1957 | 2923 | 14259 | 743 | 407 | 17 | 75 |
| NAPA1-13 | sphalerite | 1 | 97 | 98 | -21.3 | -21.4 | 70749 | 1691 | 2765 | 14653 | | 359 | 14 | |
| NAPA1-13 | sphalerite | 2 | 101 | 102 | -21.3 | -21.4 | 69991 | 1736 | 2714 | 15340 | 158 | 328 | 14 | 137 |
| NAPA1-13 | sphalerite | 1 | 104 | 105 | -21.4 | -21.5 | 54930 | 2674 | 3545 | 27287 | | 658 | 17 | |
| NAPA1-13 | sphalerite | 3 | 103 | 104 | -21.5 | -21.6 | 70897 | 1666 | 2751 | 15017 | | 383 | 13 | |
| NAPA1-13 | sphalerite | 4 | 103 | 104 | -21.5 | -21.6 | 69871 | 1217 | 3225 | 16235 | | 439 | 6 | |
| NALD1-2 | sphalerite | 1 | 124 | 125 | -20.9 | -21 | 70857 | 1696 | 3341 | 13230 | | 318 | 13 | |
| NALD1-2 | sphalerite | 2 | 116 | 117 | -20.9 | -21 | 67370 | 1894 | 3336 | 16149 | | 329 | 12 | |
| NALD1-2 | sphalerite | 1 | 101 | 102 | -21.5 | -21.4 | 74477 | 1301 | 2708 | 12054 | | 366 | 12 | |
| NALD1-2 | sphalerite | 2 | 101 | 102 | -21.5 | -21.4 | 74561 | 1586 | 2828 | 11485 | | 368 | 21 | |
| NALD1-4 | sphalerite | 1 | 105 | 106 | -19.8 | -19.9 | 61659 | 2244 | 2451 | 18578 | | 733 | 12 | |
| NALD1-4 | sphalerite | 2 | 120 | | -22.3 | -22.4 | 73697 | 1365 | 2482 | 14839 | | 503 | 12 | |
| NALD1-4 | sphalerite | 1 | 121 | 122 | -20.3 | -20.4 | 62841 | 1953 | 2595 | 18820 | | 998 | 21 | 60 |
| NALD1-4 | sphalerite | 2 | 144 | 145 | -22.3 | -22.4 | 61402 | 1405 | 3162 | 25354 | | 821 | 33 | 56 |
| NALD1-4 | sphalerite | 3 | 144 | 145 | -22.3 | -22.4 | 54302 | 1210 | 2178 | 32891 | | 688 | 43 | 89 |
| NALD1-4 | sphalerite | 4 | 144 | 145 | -22.3 | -22.4 | 69260 | 1241 | 2991 | 18512 | | 773 | 35 | 73 |
| NALD1-4 | sphalerite | 5 | 144 | 145 | -22.3 | -22.4 | 57575 | 1766 | 2795 | 28610 | | 795 | 32 | 90 |
| NALD1-4 | sphalerite | 6 | 144 | 145 | -22.3 | -22.4 | 67678 | 1518 | 3010 | 19547 | | 801 | 50 | 45 |
| NAPA1-13 | sphalerite | 1 | 100 | 101 | -21.3 | -21.2 | 68746 | 1725 | 2788 | 15914 | 69 | 503 | 10 | 275 |
| NAPA1-13 | sphalerite | 2 | 100 | 101 | -21.4 | -21.3 | 68779 | 1708 | 2722 | 16390 | | 399 | 16 | 104 |
| NAPA1-13 | sphalerite | 3 | 100 | 101 | -21.4 | -21.3 | 71173 | 1522 | 2770 | 14381 | | 408 | 10 | 183 |
| NAPA1-13 | sphalerite | 1 | 98 | 99 | -21.5 | -21.4 | 70043 | 1839 | 2666 | 15378 | | 387 | 12 | 242 |
| NAPA1-13 | sphalerite | 3 | 98 | 99 | -21.5 | -21.4 | 69547 | 1599 | 2866 | 16041 | | 377 | 14 | |
| NAPA1-13 | sphalerite | 4 | 98 | 99 | -21.5 | -21.4 | 68364 | 1764 | 2517 | 17130 | | 381 | 16 | |
| NAPA1-1 | sphalerite | 1 | 105 | 106 | -20.9 | -20.8 | 68251 | 1768 | 2746 | 15614 | | 438 | 13 | |
| NAPA1-1 | sphalerite | 2 | 105 | 106 | -20.9 | -20.8 | 62250 | 1923 | 3534 | 20203 | | 677 | 14 | |
| NAPA1-1 | sphalerite | 3 | 105 | 106 | -20.9 | -20.8 | 68117 | 1649 | 2694 | 15960 | | 409 | 14 | |
| NAPA1-1 | sphalerite | 4 | 105 | 106 | -20.9 | -20.8 | 68433 | 1818 | 2774 | 15357 | | 436 | 15 | |
| NACP1-8 | sphalerite | 1 | 111 | 112 | -22.4 | -22.5 | 70336 | 1843 | 2225 | 17068 | 591 | 612 | 16 | 128 |
| NACP1-8 | sphalerite | 2 | 111 | 112 | -22.4 | -22.5 | 69274 | 1794 | 2201 | 18043 | 719 | 641 | 18 | 59 |
| NACP1-8 | sphalerite | 3 | 111 | 112 | -22.4 | -22.5 | 66033 | 1954 | 2442 | 20077 | 1265 | 796 | 19 | 124 |
| NACP1-8 | sphalerite | 1 | 108 | 109 | -22.6 | -22.5 | 68732 | 1980 | 2358 | 18974 | | 650 | 15 | |
| NACP1-8 | sphalerite | 2 | 102 | 103 | -22.6 | -22.5 | 71203 | 1697 | 2274 | 17210 | | 578 | 15 | |
| NACP1-8 | sphalerite | 3 | 102 | 103 | -22.6 | -22.5 | 74456 | 2124 | 2231 | 13678 | | 532 | 17 | |
| NACP1-8 | sphalerite | 4 | 102 | 103 | -22.6 | -22.5 | 68668 | 1692 | 2510 | 19330 | | 657 | 15 | |

| Sample ID | Mineral Host | Fluid inclusion # | Th1 | Th2 | Tm1 | Tm2 | Na ppm | Mg ppm | K ppm | Ca ppm | Cu ppm | Sr ppm | Ba ppm | Pb ppm |
|---|---|---|---|---|---|---|---|---|---|---|---|---|---|---|
| NAEX1-2 | sphalerite | 1 | 94 | 95 | -22.5 | -22.4 | 64877 | 2404 | 2451 | 21520 | | 797 | 20 | |
| NAEX1-2 | sphalerite | 2 | 94 | 95 | -22.5 | -22.4 | 66561 | 2108 | 2392 | 20529 | | 653 | 18 | |
| NAEX1-2 | sphalerite | 3 | 94 | 95 | -22.5 | -22.4 | 69896 | 1755 | 1908 | 18343 | | 579 | 28 | |
| NAEX1-2 | sphalerite | 1 | 107 | 108 | -22.6 | -22.5 | 72111 | 1779 | 2252 | 16338 | | 482 | 15 | |
| NAEX1-2 | sphalerite | 2 | 100 | 101 | -22.6 | -22.5 | 70282 | 2200 | 2528 | 17225 | | 492 | 16 | 306 |
| NAEX1-2 | sphalerite | 3 | 112 | 113 | -22.6 | -22.5 | 68516 | 2255 | 2025 | 19051 | | 600 | 5 | 257 |
| NAEX1-2 | sphalerite | 1 | 104 | 105 | -21.7 | -21.8 | 68671 | 1830 | 2616 | 16907 | | 483 | 17 | 855 |
| NAEX1-2 | sphalerite | 2 | 104 | 105 | -21.9 | -22 | 71438 | 2145 | 1857 | 15325 | | 486 | 12 | |
| NAEX1-2 | sphalerite | 3 | 105 | 106 | -21.9 | -22 | 64149 | 2177 | 2658 | 21282 | | 694 | 16 | |
| NAEX1-2 | sphalerite | 5 | 103 | 104 | -21.7 | -21.8 | 68736 | 1532 | 2648 | 17376 | | 565 | 14 | |
| NAEX1-7 | sphalerite | 1 | 113 | 114 | -21.7 | -21.8 | 67342 | 1871 | 2220 | 18679 | | 604 | 17 | |
| NAEX1-7 | sphalerite | 2 | 107 | 108 | -21.7 | -21.8 | 62188 | 2159 | 2413 | 22808 | | 695 | 17 | 2073 |
| NAJP1-3 | sphalerite | 1 | 99 | 100 | -21.4 | -21.5 | 67785 | 1922 | 2327 | 17472 | | 526 | 20 | 79 |
| NAJP1-3 | sphalerite | 2 | 99 | 100 | -21.4 | -21.5 | 71118 | 1532 | 2088 | 15157 | | 487 | 15 | 49 |
| NALD1-4 | sphalerite | 1 | 110 | 109 | -22.2 | -22.1 | 69373 | 1973 | 2133 | 17685 | | 529 | 17 | 45 |
| NALD1-4 | sphalerite | 7 | 116 | 117 | -21.7 | -21.8 | 69096 | 1809 | 2042 | 17327 | | 531 | 16 | 60 |
| NALD1-4 | sphalerite | 8 | 110 | 111 | -21.4 | -21.5 | 67154 | 1842 | 2196 | 18016 | | 896 | 14 | 50 |
| NALD1-4 | sphalerite | 9 | 112 | 113 | -21.4 | -21.5 | 67353 | 1955 | 2464 | 17490 | | 896 | 14 | <46 |
| NALD1-4 | sphalerite | 10 | 112 | 113 | -21.4 | -21.5 | 64045 | 2263 | 2849 | 19747 | | 1014 | 16 | 152 |
| | | | | | | | | | | | | | | |
| ***Southeast Missouri district*** | | | | | | | | | | | | | | |
| MAG13A | dolomite | 1 | 157 | 158 | -22.6 | -22.5 | 91910 | | 3598 | | | | 34 | |
| MAG13A | dolomite | 1 | 154 | 155 | -22.6 | -22.5 | 91365 | | 3429 | | | | 38 | 18 |
| MAG13A | dolomite | 1 | 119 | 120 | -22.4 | -22.5 | 91338 | | 3840 | | | | 45 | 4 |
| VTSW2F | dolomite | 1 | 106 | 107 | -17.5 | -17.6 | 79154 | | 2747 | | | | 9 | 14 |
| VTSW2F | dolomite | 1 | 128 | 129 | -22.1 | -22 | 90217 | | 4076 | | | 603 | 26 | 6 |
| VTSW2F | dolomite | 1 | 130 | 131 | -6.6 | -6.7 | 38252 | | 1885 | | | | 6 | 3 |
| VTSW2F | dolomite | 2 | 124 | 125 | -22.3 | -22.4 | 91580 | | 3113 | | | 510 | 44 | |
| VTSW2F | dolomite | 1 | 105 | 106 | -19.8 | -19.9 | 85345 | | 2977 | | | 702 | 22 | 14 |
| WF2B | dolomite | 1 | 136 | 137 | -22.6 | -22.5 | 91285 | | 4359 | | | | 57 | |
| 81V22 | dolomite | 4 | 126 | 127 | -21.7 | | 90271 | | 2857 | | | | 13 | |
| VTSW2 | dolomite | 1 | 125 | 126 | -5.5 | -5.4 | 32085 | | 2032 | | | | 7 | |
| VTSW2 | dolomite | 3 | 110 | 111 | -22.4 | -22.5 | 91869 | | 2542 | | | 829 | 30 | 22 |
| VTSW2 | dolomite | 4 | 125 | 126 | -22.4 | -22.5 | 91241 | | 4109 | | | 1064 | 54 | |
| VTSW2 | dolomite | 6 | 118 | 119 | -22.4 | -22.5 | 91725 | | 3235 | | | 633 | 23 | |
| VTSW2 | dolomite | 7 | 121 | 122 | -22.4 | -22.5 | 92135 | | 3017 | | | 815 | 30 | |
| VTSW2 | dolomite | 9 | 121 | 122 | -22.4 | -22.5 | 91981 | | 2725 | | | 295 | 25 | 16 |
| VTSW2 | dolomite | 1 | 116 | 117 | -22.7 | -22.8 | 93011 | | 2817 | | | 869 | 29 | |
| VTSW2 | dolomite | 2 | 116 | 117 | -22.7 | -22.8 | 92050 | | 3993 | | | | 42 | |
| VTSW2 | dolomite | 3 | 119 | 120 | -22.7 | -22.8 | 92409 | | 3399 | | | 149 | 21 | 31 |
| VTSW2 | dolomite | 6 | 123 | 124 | -22.2 | -22.3 | 91896 | | 2013 | | | 681 | 24 | 31 |
| 35_8V22 | sphalerite | 1 | 71 | 72 | -2.5 | | 12265 | 1455 | 750 | 670 | | 47 | | |
| 35_8V22 | sphalerite | 1 | 89 | 90 | -23 | -23.1 | 74290 | 5097 | 7106 | 7614 | | 233 | | |
| 35_8V22 | sphalerite | 1 | 75 | 76 | -20.8 | -20.7 | 74671 | 1175 | 1462 | 11075 | | 270 | 9 | |
| 35_8V22 | sphalerite | 2 | 101 | 102 | -22.8 | -22.7 | 73201 | 1878 | 4507 | 14068 | | 542 | 7 | |
| 35_8V22 | sphalerite | 3 | 102 | 103 | -22.8 | -22.7 | 70976 | | 2266 | 18151 | | 496 | 17 | |
| WF2 | sphalerite | 1 | 111 | 112 | -20.4 | -20.5 | 74917 | 1220 | 2135 | 9791 | | 346 | 10 | |

| Sample ID | Mineral Host | Fluid inclusion # | Th1 | Th2 | Tm1 | Tm2 | Na ppm | Mg ppm | K ppm | Ca ppm | Cu ppm | Sr ppm | Ba ppm | Pb ppm |
|---|---|---|---|---|---|---|---|---|---|---|---|---|---|---|
| WF2 | sphalerite | 1 | 107 | 108 | -20.3 | -20.4 | 68944 | 1492 | 2358 | 14429 | | 441 | 15 | |
| MAG13 | sphalerite | 3 | 109 | 110 | -15.5 | -15.4 | 54347 | 1508 | 2014 | 14516 | | 811 | 14 | |
| MAG13 | sphalerite | 1 | 115 | 116 | -21.6 | -21.7 | 69255 | 1494 | 2433 | 16913 | | 844 | 29 | |
| MAG13 | sphalerite | 1 | 105 | 106 | -15.5 | -15.4 | 59199 | 1027 | 2004 | 11202 | | 570 | 12 | |
| MAG13 | sphalerite | 2 | 109 | 110 | -15.5 | -15.4 | 53836 | | | 14946 | | 908 | | |
| MAG13 | sphalerite | 3 | 109 | 110 | -15.5 | -15.4 | 54365 | 1797 | 2316 | 14161 | | 829 | 21 | |
| MAG13 | sphalerite | 1 | 117 | 118 | -23 | -23.1 | 75203 | 782 | 3552 | 15080 | | 595 | 20 | |
| MAG13 | sphalerite | 3 | 118 | 119 | -23.2 | -22.2 | 77395 | | 3883 | 12879 | | 619 | 29 | |
| MAG13A | sphalerite | 1 | 115 | 116 | -15.7 | -15.8 | 60113 | 1054 | 2267 | 10915 | | 718 | 19 | 165 |
| MAG13A | sphalerite | 2 | 107 | 108 | -15.6 | -15.5 | 52809 | 1640 | 2720 | 15731 | | 977 | 18 | 256 |
| MAG13A | sphalerite | 3 | 112 | 113 | -15.3 | -15.2 | 54056 | 1364 | 2562 | 14236 | | 930 | 16 | 52 |
| MAG13A | sphalerite | 4 | 104 | 105 | -15.3 | -15.2 | 52740 | 1580 | 2008 | 15588 | | 830 | 12 | 129 |
| MAG13A | sphalerite | 5 | 115 | 116 | -15.3 | -15.2 | 52107 | 1483 | 2660 | 15795 | | 921 | 15 | 52 |
| MAG13A | sphalerite | 1 | 110 | 111 | -15.3 | -15.2 | 54738 | 1014 | 2612 | 14133 | | 836 | 13 | 56 |
| MAG13A | sphalerite | 4 | 113 | 114 | -15.3 | -15.2 | 55667 | 839 | 1371 | 14385 | | 822 | 27 | |
| VTSW2E | sphalerite | 4 | 99 | 100 | -20.7 | -20.8 | 63060 | 2166 | 6080 | 16857 | | 1051 | 56 | |
| VTSW2E | sphalerite | 1 | 99 | 100 | -20.7 | -20.8 | 59528 | 4593 | 9996 | 14462 | | 339 | 6 | |
| WF2B | sphalerite | 1 | 105 | 106 | -22.5 | -22.4 | 69344 | 1955 | 2053 | 18484 | | 564 | 15 | |
| WF2B | sphalerite | 2 | 106 | 107 | -22.5 | -22.4 | 68433 | 1958 | 2271 | 19024 | | 777 | 18 | |
| | | | | | | | | | | | | | | |
| ***Tri-State district*** | | | | | | | | | | | | | | |
| TSGY2-1 | calcite | 2 | 67 | 68 | -4.2 | | 26136 | | | | | | 13 | |
| TSGY2-1 | calcite | 3 | 66 | 67 | -4.2 | | 25650 | | 986 | | | | 9 | |
| TSGY2-1 | calcite | 2 | 77 | 78 | -4.2 | | 25930 | | 685 | | | | 32 | |
| TSNC1-2 | dolomite | 1 | 108 | 109 | -18.5 | -18.6 | 81126 | | 3801 | | | 894 | 21 | |
| TSNC1-2 | dolomite | 2 | 128 | 129 | -18.5 | -18.6 | 82461 | | 2211 | | | 301 | 8 | |
| TSNC1-2 | dolomite | 3 | 128 | 129 | -18.5 | -18.6 | 81377 | | 3124 | | | | 17 | |
| TSNC1-2 | dolomite | 4 | 108 | 109 | -18.5 | -18.6 | 81617 | | 3236 | | | 1021 | 15 | |
| TSNC1-2 | dolomite | 1 | 120 | | -22 | -22.1 | 89205 | | 5326 | | | | 35 | |
| TSNC1-2 | dolomite | 2 | 120 | 121 | -22 | -22.1 | 91067 | | 2896 | | | | 49 | |
| TSNC1-2 | dolomite | 4 | 121 | 122 | -22 | -22.1 | 90559 | | 3642 | | | 1369 | 37 | |
| TSPC7-1 | dolomite | 1 | 131 | 132 | -22.9 | -22.8 | 92472 | | 3904 | | | | 64 | |
| TSPC7-1 | dolomite | 1 | 129 | 130 | -22.9 | -22.8 | 90950 | | 5857 | | | 1205 | 22 | |
| TSPC7-1 | dolomite | 1 | 122 | 123 | -22.9 | -22.8 | 92174 | | 4192 | | | 1310 | 62 | |
| TSDW2-2 | quartz | 1 | 105 | 106 | -21.8 | -21.9 | 77861 | 974 | | 11246 | | 520 | 15 | |
| TSDW2-2 | quartz | 3 | 106 | 107 | -22 | -22.1 | 71982 | 1702 | 1498 | 15804 | | 527 | 23 | |
| TSDW2-2 | quartz | 1 | 62 | 63 | -21.4 | -21.5 | 76179 | 1011 | 1746 | 11452 | | 383 | 15 | |
| TSDW2-2 | quartz | 4 | 67 | 68 | -21.7 | -21.8 | 66752 | 1050 | | 19868 | | 633 | 18 | |
| TSDW2-2 | quartz | 1 | 100 | 101 | -22 | -22.1 | 79902 | 553 | 1336 | 9786 | | 344 | 8 | |
| TSDW2-2 | quartz | 1 | 100 | 101 | -22.2 | -22.3 | 73998 | 144 | 2403 | 15960 | | 516 | 16 | |
| TSDW2-2 | quartz | 2 | 91 | 92 | -22.1 | -22.2 | 81135 | | 2178 | 9003 | | 291 | 7 | 9 |
| TSWC1-2 | quartz | 5 | 114 | 115 | -22.7 | -22.6 | 72486 | 1833 | 2218 | 16056 | | 515 | 16 | |
| TSWC1-2 | quartz | 6 | 78 | | -22.7 | -22.6 | 70966 | 1687 | 2501 | 17487 | | 585 | 16 | 1 |
| TSWC1-2 | quartz | 1 | 133 | 134 | -22.5 | -22.6 | 74041 | 441 | 2052 | 16525 | | 471 | 13 | 1 |
| TSWC1-2 | quartz | 2 | 109 | 110 | -22.6 | -22.7 | 80244 | 962 | 2527 | 10046 | | 341 | 13 | 2 |
| TSWC1-2 | quartz | 5 | 112 | 113 | -22.6 | -22.7 | 79650 | 714 | 1788 | 11214 | | 371 | 14 | |
| TSWC1-2 | quartz | 1 | 140+ | | -22.1 | -22 | 78634 | 705 | 2466 | 10639 | | 323 | 15 | 3 |

| Sample ID | Mineral Host | Fluid inclusion # | Th1 | Th2 | Tm1 | Tm2 | Na ppm | Mg ppm | K ppm | Ca ppm | Cu ppm | Sr ppm | Ba ppm | Pb ppm |
|---|---|---|---|---|---|---|---|---|---|---|---|---|---|---|
| TSWC1-2 | quartz | 2 | 86 | 87 | -22.1 | -22 | 76550 | 51 | 1794 | 13859 | | 441 | 17 | 2 |
| TSWC1-2 | quartz | 3 | 122 | 123 | -22.4 | -22.5 | 75741 | 303 | 2371 | 14806 | | 430 | 17 | |
| TSWC1-2 | quartz | 4 | 139 | 140 | -22.4 | -22.5 | 76776 | 264 | 2267 | 13988 | | 417 | 17 | |
| TSBS3-2 | sphalerite | 2 | 98 | 99 | -15.8 | -15.7 | 52667 | 1764 | 2339 | 16562 | | 923 | 18 | |
| TSBS3-2 | sphalerite | 3 | 108 | 109 | -15.8 | -15.7 | 50816 | 1839 | 2943 | 17772 | | 878 | 12 | |
| TSBS3-2 | sphalerite | 5 | 113 | 114 | -15.8 | -15.7 | 53875 | 1271 | 1804 | 16582 | | 831 | 15 | |
| TSBS3-2 | sphalerite | 6 | 101 | 102 | -15.8 | -15.7 | 49565 | 1761 | 3509 | 18686 | | 812 | 10 | |
| TSBS3-2 | sphalerite | 7 | 94 | 95 | -15.9 | -15.8 | 58859 | 1455 | | 12305 | | 1018 | 11 | |
| TSBS3-2 | sphalerite | 10 | 97 | 98 | -15.8 | -15.7 | 50822 | 1765 | 2309 | 18566 | | 916 | 22 | |
| TSBS3-2 | sphalerite | 1 | 105 | 106 | -20.8 | -20.9 | 73195 | 1026 | 1527 | 12668 | | 881 | 23 | |
| TSBS3-2 | sphalerite | 2 | 100 | 101 | -21.1 | -21 | 60946 | 1716 | | 22971 | | 884 | 16 | |
| TSNC1-1 | sphalerite | 4 | 99 | 100 | -22.6 | -22.7 | 80663 | 3856 | | | | 628 | | 785 |
| TSNC1-1 | sphalerite | 5 | 110 | 111 | -22.6 | -22.7 | 66637 | 1835 | 4498 | 18719 | | 837 | 27 | 670 |
| TSNC1-1 | sphalerite | 6 | 94 | 95 | -22.6 | -22.7 | 62986 | 5497 | | 18940 | | 446 | 26 | 155 |
| TSDW2-8 | sphalerite | 1 | 101 | 102 | -22.6 | -22.7 | 65993 | 3024 | | 20934 | | 715 | 15 | 34 |
| TSDW2-8 | sphalerite | 2 | 101 | 102 | -22.6 | -22.7 | 65708 | 1916 | 2082 | 22320 | | 484 | 10 | 50 |
| TSDW2-8 | sphalerite | 1 | 99 | 100 | -22.9 | -23 | 70672 | 2256 | 2581 | 17564 | | 570 | 20 | 22 |
| TSDW2-8 | sphalerite | 2 | 99 | 100 | -23 | -23.1 | 70593 | 2283 | 2664 | 17767 | | 573 | 20 | 19 |
| TSDW2-8 | sphalerite | 1 | 93 | 94 | -22.9 | -23 | 66186 | 2867 | 2725 | 20598 | | 792 | 9 | 18 |
| TSDW2-8 | sphalerite | 1 | 91 | 92 | -22.6 | -22.7 | 66889 | 2247 | 3025 | 20090 | | 536 | 16 | |
| TSDW2-8 | sphalerite | 1 | 97 | 98 | -22.6 | -22.7 | 72095 | 1985 | 2313 | 16224 | | 499 | 16 | 13 |
| TSBS5-2 | sphalerite | 1 | 118 | 119 | -22.1 | -22.2 | 66299 | 1577 | 3187 | 19773 | | 770 | 39 | 868 |
| TSBS5-2 | sphalerite | 3 | 116 | 117 | -22.1 | -22.2 | 67064 | 1603 | 2849 | 19462 | | 768 | 29 | 480 |
| TSBS5-2 | sphalerite | 4 | 118 | 119 | -22.1 | -22.2 | 70243 | | | 18535 | | 811 | 47 | 1165 |
| TSCM2-1 | sphalerite | 2 | 112 | 113 | -16.8 | -16.9 | 57636 | 2073 | 2124 | 14759 | | 1009 | 15 | 435 |
| TSCM2-1 | sphalerite | 3 | 112 | 113 | -17.1 | -17.2 | 59599 | 1579 | 2634 | 14250 | | 823 | 11 | |
| TSCM2-1 | sphalerite | 4 | 112 | 113 | -16.8 | -16.9 | 56519 | 1646 | 1865 | 16662 | | 862 | 17 | |
| TSCM2-1 | sphalerite | 1 | 114 | 115 | -18.1 | -18.2 | 60238 | 1580 | 2230 | 16579 | | 867 | 10 | |
| TSCM2-1 | sphalerite | 2 | 115 | 116 | -18.3 | -18.4 | 60339 | 1917 | | 16440 | | 919 | 22 | |
| TSCM2-1 | sphalerite | 3 | 114 | 115 | -18.1 | -18.2 | 62315 | 1457 | 2136 | 14902 | | 878 | 12 | |
| TSDW2-8 | sphalerite | 1 | 106 | 107 | -23.3 | -23.4 | 75745 | 1907 | 2129 | 14684 | | 489 | 15 | 77 |
| TSDW2-8 | sphalerite | 2 | 105 | 106 | -23.3 | -23.4 | 75436 | 1752 | 2315 | 15089 | | 481 | 18 | 21 |
| TSDW2-8 | sphalerite | 3 | 105 | 106 | -23.3 | -23.4 | 72634 | 1961 | 2165 | 17386 | | 588 | 19 | 50 |
| TSDW2-9 | sphalerite | 1 | 107 | 108 | -23.1 | -23.2 | 67970 | 1479 | 2541 | 20345 | 1586 | 671 | 19 | 104 |
| TSDW2-9 | sphalerite | 2 | 108 | 109 | -23.1 | -23.2 | 71773 | 1760 | 1731 | 16931 | 1655 | 715 | 19 | 105 |
| TSDW2-9 | sphalerite | 3 | 103 | 104 | -23.1 | -23.2 | 72193 | 2002 | 2113 | 16114 | 1486 | 605 | 16 | 167 |
| TSDW2-9 | sphalerite | 4 | 103 | 104 | -23.1 | -23.2 | 68693 | 2193 | 2306 | 18975 | 1449 | 595 | 18 | 130 |
| TSDW2-9 | sphalerite | 5 | 103 | 104 | -23.1 | -23.2 | 67682 | 2119 | 2719 | 20903 | 1166 | 584 | 15 | 956 |
| TSGY2-3 | sphalerite | 1 | 108 | 109 | -22.9 | -23 | 64576 | 1903 | 2870 | 23235 | | 982 | 28 | |
| TSGY2-3 | sphalerite | 2 | 108 | 109 | -23.1 | -23 | 69321 | 1713 | 2165 | 19977 | | 804 | 27 | |
| TSGY2-3 | sphalerite | 3 | 107 | 108 | -23.2 | -23.1 | 66980 | 1436 | 3126 | 21984 | | 952 | 32 | |
| TSPC2-1 | sphalerite | 1 | 118 | 119 | -23 | -23.1 | 71869 | 1965 | 1878 | 17604 | | 622 | 14 | 259 |
| TSPC2-1 | sphalerite | 2 | 118 | 119 | -23.1 | -23.2 | 68792 | 1874 | | 20848 | | 634 | 17 | 279 |
| TSPC2-1 | sphalerite | 4 | 122 | 123 | -23 | -23.1 | 69778 | 1981 | 2032 | 19389 | | 624 | 23 | 233 |
| TSPC2-1 | sphalerite | 5 | 121 | 122 | -23.1 | -23.2 | 70074 | 2533 | | 18846 | | 723 | 19 | |
| TSPC2-1 | sphalerite | 6 | 120 | 121 | -23 | -23.1 | 66349 | 2108 | 4752 | 20481 | | 635 | 16 | 637 |
| TSPC2-1 | sphalerite | 1 | 106 | 107 | -22.7 | -22.8 | 72891 | 2561 | | 15401 | | 605 | 9 | |

| Sample ID | Mineral Host | Fluid inclusion # | Th1 | Th2 | Tm1 | Tm2 | Na ppm | Mg ppm | K ppm | Ca ppm | Cu ppm | Sr ppm | Ba ppm | Pb ppm |
|---|---|---|---|---|---|---|---|---|---|---|---|---|---|---|
| TSPC2-1 | sphalerite | 6 | 105 | 106 | -22.7 | -22.8 | 71640 | 1703 | 2639 | 16975 | | 628 | 14 | |
| TSOR2-3 | sphalerite | 1 | 109 | 110 | -23.1 | -23.2 | 71694 | 2210 | 2115 | 17479 | | 620 | 23 | |
| TSPC2-1 | sphalerite | 1 | 108 | 109 | -22.7 | -22.8 | 69861 | | | 21221 | | 786 | 19 | |
| TSPC2-1 | sphalerite | 2 | 108 | 109 | -22.7 | -22.8 | 68879 | 1610 | 2505 | 19597 | | 812 | 41 | |
| TSPC2-1 | sphalerite | 3 | 108 | 109 | -22.7 | -22.8 | 68057 | 1316 | 3894 | 19794 | | 839 | 43 | 423 |
| TSPC2-1 | sphalerite | 1 | 122 | 123 | -22.6 | -22.7 | 71917 | 1250 | 3601 | 16418 | | 692 | 33 | |
| TSPC2-1 | sphalerite | 2 | 112 | 113 | -22.6 | -22.7 | 65006 | 1563 | 2992 | 22552 | | 973 | 41 | 69 |
| TSPC2-1 | sphalerite | 1 | 112 | 113 | -22.8 | -22.9 | 72299 | 1590 | 2301 | 17009 | | 599 | 15 | |
| TSPC2-1 | sphalerite | 2 | 111 | 112 | -22.8 | -22.9 | 70626 | 1823 | 2328 | 18165 | | 645 | 16 | |
| TSPC2-1 | sphalerite | 3 | 111 | 112 | -22.8 | -22.9 | 63950 | 2348 | 2584 | 23294 | | 770 | 17 | |
| TSTR1-7 | sphalerite | 1 | 107 | 108 | -21.2 | -21.3 | 70485 | 1533 | 2352 | 14925 | | 721 | 21 | 4 |
| TSTR1-7 | sphalerite | 2 | 111 | 112 | -21.2 | -21.3 | 64972 | 2097 | 2933 | 18603 | | 1009 | 20 | 7 |
| TSTR1-7 | sphalerite | 4 | 109 | 110 | -21.2 | -21.3 | 70529 | 1329 | 2197 | 15279 | | 675 | 18 | 73 |
| TSTR1-7 | sphalerite | 5 | 112 | 113 | -21.2 | -21.3 | 68691 | 1939 | 2693 | 15690 | | 751 | 24 | 113 |
| TSTR1-7 | sphalerite | 6 | 107 | 108 | -21.2 | -21.3 | 69952 | 1549 | 2645 | 15202 | | 684 | 21 | 32 |
| TSTR1-7 | sphalerite | 7 | 109 | 110 | -21.2 | -21.3 | 67927 | 1812 | 2467 | 16807 | | 707 | 18 | 12 |
| TSTR1-7 | sphalerite | 8 | 109 | 110 | -21.2 | -21.3 | 65895 | 1970 | 2946 | 17796 | | 848 | 30 | 476 |
| TSTR1-7 | sphalerite | 9 | 110 | 111 | -21.2 | -21.3 | 63897 | 2899 | 2452 | 18924 | | 798 | 20 | 109 |
| TSTR1-7 | sphalerite | 10 | 111 | 112 | -20.6 | -20.7 | 64852 | 1833 | 2630 | 17937 | | 901 | 19 | |
| TSTR1-7 | sphalerite | 11 | 107 | 108 | -21.2 | -21.3 | 63624 | 2507 | 3032 | 19226 | | 960 | 16 | |
| TSWB3-9 | sphalerite | 1 | 115 | 116 | -23.1 | -23.2 | 73872 | 1586 | 2448 | 16182 | | 551 | 16 | |
| TSWB3-9 | sphalerite | 2 | 117 | 118 | -23.1 | -23.2 | 71405 | 1737 | 1941 | 18519 | | 647 | 15 | 173 |
| TSWB3-9 | sphalerite | 6 | 119 | 120 | -23.1 | -23.2 | 73733 | 1413 | 1663 | 16990 | | 713 | 15 | |
| TSWB3-9 | sphalerite | 8 | 118 | 119 | -23.1 | -23.2 | 73393 | 1540 | 2252 | 16796 | | 584 | 22 | |
| TSWB3-9 | sphalerite | 9 | 123 | 124 | -23.1 | -23.2 | 72760 | 1595 | 2888 | 16821 | | 655 | 12 | |
| TSWB3-9 | sphalerite | 12 | 119 | 120 | -23.1 | -23.2 | 73924 | 1399 | 2660 | 16194 | | 637 | 21 | 249 |
| TSBS5-2 | sphalerite | 1 | 109 | 110 | -22.4 | -22.5 | 71937 | 1651 | 2477 | 16230 | | 580 | 16 | 116 |
| TSBS5-2 | sphalerite | 1 | 120 | 121 | -12.3 | -12.4 | 44203 | 1629 | 1793 | 14391 | | 722 | 13 | |
| TSBS5-2 | sphalerite | 3 | 119 | 120 | -12.3 | -12.4 | 47925 | 1020 | 1733 | 11935 | | 633 | 14 | |
| TSBS5-2 | sphalerite | 1 | 130 | 131 | -22.9 | -22.8 | 69120 | 1711 | 2965 | 19216 | | 705 | 40 | |
| TSBS5-2 | sphalerite | 2 | 130 | 131 | -22.9 | -22.8 | 66401 | 2105 | 3808 | 20548 | | 756 | 28 | |
| TSBS5-2 | sphalerite | 3 | 130 | 131 | -22.9 | -22.8 | 67814 | 1538 | 3083 | 20540 | | 767 | 36 | |
| TSBS5-2 | sphalerite | 4 | 130 | 131 | -22.9 | -22.8 | 66229 | 1761 | 3185 | 21506 | | 916 | 50 | |
| TSBS5-2 | sphalerite | 5 | 130 | 131 | -22.9 | -22.8 | 67042 | 1508 | 2872 | 21410 | | 802 | 41 | |
| TSBS5-2 | sphalerite | 1 | 110 | 111 | -22.4 | -22.5 | 67926 | 1891 | 2728 | 19327 | | 694 | 16 | 166 |
| TSBS5-2 | sphalerite | 2 | 108 | 109 | -22.4 | -22.5 | 71247 | 1777 | 2602 | 16583 | | 604 | 17 | 42 |
| TSBS5-2 | sphalerite | 3 | 107 | 108 | -22.4 | -22.5 | 69608 | 1799 | 2201 | 18295 | | 660 | 19 | 202 |
| TSBS5-2 | sphalerite | 4 | 111 | 112 | -22.4 | -22.5 | 65767 | 2153 | 2742 | 20862 | | 792 | 18 | |
| TSBS5-2 | sphalerite | 5 | 108 | 109 | -22.4 | -22.5 | 68036 | 2032 | 2265 | 19353 | | 678 | 18 | |
| TSBS5-2 | sphalerite | 6 | 110 | 111 | -22.4 | -22.5 | 68775 | 1756 | 2359 | 18986 | | 697 | 22 | |
| TSCM2-1 | sphalerite | 1 | 105 | 106 | -18.3 | -18.2 | 58741 | 2197 | 2675 | 16959 | | 975 | 17 | |
| TSCM2-1 | sphalerite | 2 | 105 | 106 | -18.3 | -18.2 | 59822 | 2107 | 2272 | 16233 | | 1189 | 15 | 144 |
| TSCM2-1 | sphalerite | 3 | 105 | 106 | -18.1 | -18 | 57865 | 1842 | 2545 | 17838 | 812 | 966 | 17 | 78 |
| TSCM2-1 | sphalerite | 4 | 106 | 107 | -18.3 | -18.2 | 59328 | 1335 | 2909 | 17511 | | 925 | 18 | |
| TSCM2-1 | sphalerite | 5 | 107 | 108 | -18.3 | -18.2 | 58350 | 1893 | 2300 | 17995 | | 991 | 18 | 117 |
| TSCM2-1 | sphalerite | 7 | 109 | 110 | -18.1 | -18 | 57053 | 2407 | 2810 | 17580 | | 1001 | 16 | |
| TSCM2-1 | sphalerite | 2 | 103 | 104 | -18 | -18.1 | 59155 | 1849 | 2347 | 16801 | | 935 | 16 | 15 |

| Sample ID | Mineral Host | Fluid inclusion # | Th1 | Th2 | Tm1 | Tm2 | Na ppm | Mg ppm | K ppm | Ca ppm | Cu ppm | Sr ppm | Ba ppm | Pb ppm |
|---|---|---|---|---|---|---|---|---|---|---|---|---|---|---|
| TSCM2-1 | sphalerite | 1 | 105 | 106 | -18 | -17.9 | 66489 | 1491 | 1589 | 11087 | | 554 | 10 | 66 |
| TSCM2-1 | sphalerite | 2 | 109 | 110 | -18 | -17.9 | 59941 | 1760 | 2446 | 15880 | | 925 | 18 | |
| TSCM2-1 | sphalerite | 3 | 103 | 104 | -18 | -17.9 | 58621 | 1880 | 2738 | 16709 | | 950 | 12 | 53 |
| TSCM2-1 | sphalerite | 5 | 109 | 110 | -18 | -17.9 | 61293 | 1667 | 2449 | 14819 | | 849 | 17 | |
| TSNC1-2 | sphalerite | 1 | 96 | 97 | -23.1 | -23 | 69613 | 2041 | 2472 | 19146 | | 638 | 18 | |
| TSNC1-2 | sphalerite | 2 | 98 | 99 | -23.1 | -23 | 66942 | 1962 | 2525 | 21631 | | 704 | 19 | |
| TSNC1-2 | sphalerite | 3 | 98 | 99 | -23.1 | -23 | 71868 | 1392 | 2337 | 18097 | | 622 | 20 | |
| TSNC1-2 | sphalerite | 4 | 101 | 102 | -23.1 | -23 | 69214 | 1931 | 2532 | 19605 | | 673 | 19 | |
| TSNC1-2 | sphalerite | 5 | 97 | 98 | -23.1 | -23 | 68669 | 1900 | 2931 | 19829 | | 738 | 20 | |
| TSNC1-2 | sphalerite | 6 | 96 | 97 | -23.1 | -23 | 70551 | 1669 | 2940 | 18460 | | 682 | 20 | |
| TSNC1-2 | sphalerite | 8 | 101 | 102 | -23.1 | -23 | 68973 | 1768 | 2602 | 20018 | | 660 | 17 | |
| TSNC1-2 | sphalerite | 1 | 94 | 95 | -22.4 | -22.5 | 70606 | 1638 | 2279 | 17555 | | 661 | 14 | |
| TSWB3-9 | sphalerite | 1 | 120 | 121 | -22.9 | -22.8 | 68984 | 2356 | 2426 | 18755 | | 795 | 15 | |
| TSWB3-9 | sphalerite | 2 | 120 | 121 | -22.9 | -22.8 | 67676 | 2168 | 2123 | 20464 | | 739 | 19 | |
| TSWB3-9 | sphalerite | 4 | 121 | 122 | -22.9 | -22.8 | 68793 | 2089 | 2218 | 19500 | | 719 | 17 | |
| TSWB3-9 | sphalerite | 5 | 120 | 120 | -22.9 | -22.8 | 66713 | 2416 | 2185 | 20978 | | 701 | 21 | |
| TSWB3-9 | sphalerite | 6 | 121 | 122 | -22.9 | -22.8 | 67633 | 2372 | 2478 | 19994 | | 703 | 19 | |
| TSWB3-9 | sphalerite | 7 | 120 | 121 | -22.9 | -22.8 | 69757 | 2008 | 2410 | 18647 | | 640 | 16 | |
| TSTR1-7 | sphalerite | 2 | 107 | 108 | -21.4 | -21.5 | 65711 | 1900 | 2399 | 19142 | | 855 | 21 | |
| TSTR1-7 | sphalerite | 3 | 109 | 110 | -21.2 | -21.3 | 65971 | 1808 | 2534 | 18412 | | 805 | 25 | 182 |
| TSTR1-7 | sphalerite | 5 | 110 | 111 | -21.2 | -21.3 | 65488 | 1949 | 2581 | 18672 | | 866 | 24 | |
| TSTR1-7 | sphalerite | 6 | 111 | 112 | -20.7 | -20.8 | 60241 | 1910 | 2756 | 22184 | | 947 | 20 | 21 |
| TSTR1-7 | sphalerite | 7 | 110 | 111 | -20.7 | -20.8 | 62942 | 1885 | 2584 | 19867 | | 930 | 21 | |
| TSTR1-7 | sphalerite | 8 | 107 | 108 | -20.7 | -20.8 | 61334 | 1847 | 2697 | 21278 | | 998 | 18 | |
| TSTR1-7 | sphalerite | 9 | 110 | 111 | -20.7 | -20.8 | 65523 | 2009 | 2407 | 17524 | | 812 | 20 | 276 |
| TSTR1-7 | sphalerite | 10 | 110 | 111 | -20.7 | -20.8 | 62395 | 2038 | 2386 | 20309 | | 896 | 27 | 110 |
| TSTR1-7 | sphalerite | 11 | 111 | 112 | -22.4 | -22.5 | 58873 | 2590 | 2814 | 26325 | | 1082 | 35 | 10 |
| TSTR1-7 | sphalerite | 12 | 110 | 111 | -22.4 | -22.5 | 66298 | 2744 | 2802 | 19364 | | 985 | 32 | 62 |
| TSTR1-7 | sphalerite | 13 | 111 | 112 | -22.4 | -22.5 | 66527 | 2432 | 2453 | 19837 | | 993 | 21 | 165 |
| TSTR1-7 | sphalerite | 14 | 111 | 112 | -21.8 | -21.9 | 66273 | 1797 | 2533 | 19708 | | 707 | 27 | 63 |
| TSTR1-7 | sphalerite | 15 | 108 | 109 | -22.9 | -22.8 | 59962 | 2179 | 2544 | 26975 | | 1139 | 27 | 15 |
| TSTR1-7 | sphalerite | 17 | 112 | 113 | -22.9 | -22.8 | 68953 | 1593 | 2723 | 19676 | | 757 | 28 | 87 |
| TSWC1-3 | sphalerite | 1 | 101 | 102 | -16.4 | -16.5 | 54552 | 2009 | 1813 | 16753 | | 1063 | 9 | |
| TSWC1-3 | sphalerite | 2 | 99 | 100 | -16.4 | -16.5 | 54301 | 2122 | | 18093 | | 1031 | 8 | |
| TSWC1-3 | sphalerite | 3 | 118 | 119 | -16.4 | -16.5 | 50220 | 2418 | 2080 | 19906 | | 1151 | 15 | |
| TSWC1-3 | sphalerite | 4 | 101 | 102 | -16.4 | -16.5 | 53847 | 1805 | | 17879 | | 1074 | 15 | 145 |
| TSWC1-3 | sphalerite | 5 | 101 | 102 | -16.4 | -16.5 | 58071 | 1776 | 2020 | 13675 | 372 | 1114 | 10 | 132 |
| TSWC1-3 | sphalerite | 6 | 101 | 102 | -16.4 | -16.5 | 54213 | 2089 | 2573 | 16384 | 387 | 1126 | 14 | 220 |
| TSWC1-3 | sphalerite | 7 | 101 | 102 | -16.4 | -16.5 | 52855 | 2043 | 3067 | 17465 | 755 | 955 | 17 | 296 |
| TSWC1-3 | sphalerite | 8 | 101 | 102 | -16.4 | -16.5 | 54121 | 1629 | 1743 | 17858 | 583 | 872 | 10 | 214 |

* Th = homogenization temperature

** Tm = last ice melting temperature

# Appendix III

## LA-ICP-MS Elemental Composition Analyses of Sphalerite from Ozark MVT Deposits

| Sample ID | Mineral | FI# | Fe ppm | Cu ppm | Zn ppm | Cd ppm | Pb ppm |
|---|---|---|---|---|---|---|---|
| NACP1-8 | sphalerite | 1 | 1119 | 22 | 664230 | 6395 | 4 |
| NACP1-8 | sphalerite | 2 | 1115 | 11 | 663841 | 6836 | 1 |
| NACP1-8 | sphalerite | 3 | 1010 | 91 | 664440 | 6177 | 21 |
| NACP1-8 | sphalerite | 1 | 963 | 179 | 664913 | 5562 | 48 |
| NACP1-8 | sphalerite | 2 | 951 | 100 | 664662 | 5964 | 50 |
| NACP1-8 | sphalerite | 3 | 1001 | 141 | 664225 | 6333 | 69 |
| NACP1-8 | sphalerite | 1 | 1036 | 89 | 664993 | 5495 | 12 |
| NACP1-8 | sphalerite | 2 | 977 | 99 | 665652 | 4829 | 9 |
| NACP1-8 | sphalerite | 3 | 999 | 73 | 664026 | 6707 | 12 |
| NAPA1-13B | sphalerite | 1 | 293 | 159 | 667171 | 3772 | 49 |
| NAPA1-13B | sphalerite | 2 | 299 | 114 | 667109 | 3934 | 30 |
| NAPA1-13B | sphalerite | 3 | 314 | 282 | 667173 | 3571 | 94 |
| NAPA1-13B | sphalerite | 4 | 352 | 608 | 666901 | 3368 | 190 |
| NAEX1-8 | sphalerite | 1 | 1548 | 117 | 665379 | 4397 | 22 |
| NAEX1-8 | sphalerite | 2 | 1403 | 158 | 663469 | 6291 | 53 |
| NAEX1-8 | sphalerite | 1 | 1703 | 144 | 665074 | 4515 | 29 |
| NAEX1-8 | sphalerite | 2 | 1695 | 151 | 664893 | 4735 | 33 |
| NALD1-2 | sphalerite | 1 | 502 | 827 | 666213 | 3679 | 109 |
| NALD1-2 | sphalerite | 1 | 375 | 9 | 666633 | 4553 | |
| NAPA1-13 | sphalerite | 1 | 417 | 45 | 666576 | 4518 | 4 |
| NAPA1-13 | sphalerite | 2 | 411 | 36 | 667137 | 3885 | 3 |
| NAPA1-13 | sphalerite | 3 | 419 | 35 | 666205 | 4958 | 4 |
| NAPA1-13 | sphalerite | 4 | 415 | 40 | 667014 | 3967 | 3 |
| NACP1-8 | sphalerite | 1 | 987 | 17 | 664546 | 6174 | 4 |
| NACP1-8 | sphalerite | 3 | 1009 | 18 | 663326 | 7534 | 9 |
| NACP1-8 | sphalerite | 4 | 1042 | 19 | 664570 | 6086 | 5 |
| NAPA1-13 | sphalerite | 1 | 453 | 8 | 666219 | 4897 | |
| NAPA1-13 | sphalerite | 1 | 419 | 445 | 666052 | 4384 | 134 |
| NAPA1-13 | sphalerite | 1 | 468 | 307 | 666145 | 4265 | 80 |
| NAPA1-13 | sphalerite | 2 | 445 | 323 | 666515 | 4041 | 64 |
| NAPA1-13 | sphalerite | 3 | 513 | 318 | 666854 | 3686 | 67 |
| NAJP1-3 | sphalerite | 1 | 407 | 8 | 665428 | 5909 | 1 |
| NAJP1-3 | sphalerite | 2 | 430 | 6 | 664938 | 6401 | |
| NAJP1-3 | sphalerite | 4 | 431 | 9 | 664903 | 6423 | |
| NAJP1-3 | sphalerite | 5 | 476 | 10 | 665265 | 5912 | |
| NAJP1-3 | sphalerite | | 388 | 6 | 665013 | 6416 | |
| NAJP1-3o | sphalerite | 1 | 627 | 197 | 667442 | 2996 | 15 |
| NAMC1-1 | sphalerite | 1 | 880 | 150 | 666026 | 4448 | 17 |
| NAMC1-1 | sphalerite | 2 | 1143 | 14 | 664030 | 6543 | 4 |
| NAMC1-1 | sphalerite | 3 | 987 | 51 | 665054 | 5561 | 12 |
| NAMC1-1 | sphalerite | 4 | 934 | 113 | 665531 | 4992 | 4 |
| NAMC1-1 | sphalerite | 5 | 884 | 13 | 664396 | 6501 | 4 |
| NAMC1-1 | sphalerite | 1 | 1109 | 95 | 662847 | 7725 | 46 |
| NAMC1-1 | sphalerite | 2 | 1150 | 101 | 662311 | 8439 | 57 |

| Sample ID | Mineral | FI# | Fe ppm | Cu ppm | Zn ppm | Cd ppm | Pb ppm |
|---|---|---|---|---|---|---|---|
| NAMC1-1 | sphalerite | 4 | 1048 | 89 | 661426 | 9447 | 86 |
| NAMC1-1 | sphalerite | | 1274 | 79 | 661803 | 8905 | 55 |
| NAMC1-1 | sphalerite | | 1417 | 97 | 662127 | 8358 | 6 |
| NAEX1-7 | sphalerite | 2 | 744 | 229 | 667206 | 3037 | 15 |
| NAEX1-7 | sphalerite | 1 | 752 | 80 | 667147 | 3313 | 12 |
| NAEX1-7 | sphalerite | 1 | 1078 | 2 | 665367 | 5016 | |
| NAEX1-7 | sphalerite | 2 | 1120 | 1 | 665306 | 5066 | |
| NAEX1-7 | sphalerite | 3 | 1125 | 1 | 665327 | 5020 | |
| NAEX1-7 | sphalerite | 4 | 1163 | 1 | 665409 | 4874 | |
| NAEX1-7 | sphalerite | | 886 | 1 | 666163 | 4373 | |
| NAEX1-7 | sphalerite | | 802 | 1018 | 667749 | 1463 | 5 |
| NAEX1-7 | sphalerite | 1 | 905 | 162 | 667751 | 2257 | 5 |
| NAEX1-7 | sphalerite | | 949 | 44 | 667685 | 2458 | 1 |
| NAEX1-7 | sphalerite | | 896 | 27 | 668042 | 2140 | 1 |
| NAEX1-7 | sphalerite | | 1011 | 23 | 667659 | 2461 | 1 |
| NACP1-8 | sphalerite | 1 | 1101 | 34 | 663148 | 7451 | 2 |
| NACP1-8 | sphalerite | 2 | 1151 | 26 | 663353 | 7221 | 1 |
| NACP1-8 | sphalerite | 1 | 1191 | 12 | 663519 | 6941 | 7 |
| NACP1-8 | sphalerite | 2 | 1043 | 20 | 664498 | 5885 | 4 |
| NACP1-8 | sphalerite | 4 | 1166 | 92 | 664339 | 5840 | 13 |
| NAEX1-14 | sphalerite | 1 | 866 | 277 | 667645 | 2188 | 4 |
| NAEX1-14 | sphalerite | 2 | 965 | 463 | 667633 | 1931 | 5 |
| NAEX1-14 | sphalerite | 3 | 924 | 100 | 667275 | 2831 | 12 |
| NAEX1-2 | sphalerite | 1 | 713 | 46 | 666948 | 3382 | 9 |
| NAEX1-2 | sphalerite | 2 | 735 | 64 | 666816 | 3522 | 14 |
| NAEX1-2 | sphalerite | 3 | 727 | 62 | 666997 | 3282 | 12 |
| NAJP1-10 | sphalerite | 1 | 891 | 24 | 665230 | 5366 | |
| NAJP1-10 | sphalerite | 2 | 881 | 34 | 664733 | 5865 | 1 |
| NAJP1-10 | sphalerite | 3 | 804 | 29 | 664857 | 5894 | 1 |
| NAJP1-10 | sphalerite | 4 | 842 | 46 | 664056 | 6711 | |
| NAJP1-10 | sphalerite | 4 | 758 | 72 | 664159 | 6659 | 2 |
| NAJP1-10 | sphalerite | 1 | 992 | 94 | 659735 | 11122 | 23 |
| NAJP1-10 | sphalerite | 2 | 968 | 77 | 660436 | 10843 | 3 |
| NAJP1-10 | sphalerite | 3 | 1028 | 33 | 663823 | 6751 | 1 |
| NAJP1-10 | sphalerite | | 1303 | 169 | 661351 | 8962 | 1 |
| NAJP1-10 | sphalerite | | 1201 | 174 | 661581 | 9030 | 1 |
| NAJP1-10 | sphalerite | | 1295 | 178 | 661519 | 9157 | 1 |
| NAJP1-10 | sphalerite | | 1363 | 108 | 663425 | 6794 | 10 |
| NAJP1-10 | sphalerite | | 760 | 246 | 667706 | 2453 | 4 |
| NAJP1-10 | sphalerite | | 750 | 209 | 667553 | 2702 | 8 |
| NALB1-1 | sphalerite | 1 | 808 | 1 | 664164 | 6805 | |
| NALB1-1 | sphalerite | 2 | 1080 | 1 | 663823 | 6851 | |
| NALB1-1 | sphalerite | 3 | 878 | | 663647 | 7314 | |
| NALB1-1 | sphalerite | 1 | 457 | 16 | 665318 | 5846 | 1 |
| NALB1-1 | sphalerite | 2 | 457 | 16 | 665318 | 5846 | 1 |
| NALD1-4 | sphalerite | 4 | 397 | 451 | 667192 | 3116 | 63 |
| NALD1-4 | sphalerite | | 457 | 16 | 665318 | 5846 | 1 |
| NALD1-4 | sphalerite | | 390 | 418 | 667278 | 3145 | 59 |
| NAMC1-1 | sphalerite | 1 | 1488 | 38 | 660860 | 9695 | 12 |

| Sample ID | Mineral | FI# | Fe ppm | Cu ppm | Zn ppm | Cd ppm | Pb ppm |
|---|---|---|---|---|---|---|---|
| NAMC1-1 | sphalerite | 2 | 1526 | 80 | 659234 | 11365 | 15 |
| NAMC1-1 | sphalerite | 3 | 1784 | 98 | 660751 | 9401 | 14 |
| NAMC1-1 | sphalerite | 4 | 1607 | 42 | 660136 | 10373 | 11 |
| NAMC1-1 | sphalerite | 6 | 1765 | 132 | 660242 | 9993 | 19 |
| NAMC1-1 | sphalerite | | 1343 | 194 | 660450 | 10108 | 2 |
| NAMC1-1 | sphalerite | | 1359 | 203 | 660408 | 10222 | 2 |
| NAMC1-1 | sphalerite | | 1663 | 113 | 661188 | 9072 | 11 |
| NAMC1-1 | sphalerite | | 1702 | 120 | 661048 | 9179 | 10 |
| NAMC1-1 | sphalerite | | 1150 | 192 | 663960 | 6356 | 31 |
| NAMC1-1 | sphalerite | | 1040 | 152 | 664491 | 5920 | 17 |
| NAMC1-1 | sphalerite | 1 | 1008 | 46 | 665051 | 5443 | 11 |
| NAMC1-1 | sphalerite | 2 | 943 | 21 | 664590 | 6092 | 3 |
| NAMC1-1 | sphalerite | 1 | 1227 | 17 | 663752 | 6727 | 1 |
| NAMC1-1 | sphalerite | 2 | 1456 | 52 | 661757 | 8673 | 19 |
| NAMC1-1 | sphalerite | 3 | 1524 | 31 | 660397 | 10244 | 24 |
| NAMC1-1 | sphalerite | 4 | 1711 | 25 | 659989 | 10484 | 19 |
| NAMC1-1 | sphalerite | 2 | 1070 | 91 | 663476 | 7094 | 44 |
| NAMC1-1 | sphalerite | 3 | 1116 | 60 | 662961 | 7698 | 25 |
| NAMC1-1 | sphalerite | 4 | 1363 | 21 | 662119 | 8410 | 11 |
| NAMC1-1 | sphalerite | 5 | 1011 | 10 | 663695 | 7048 | 6 |
| NAMC1-1 | sphalerite | 2 | 1839 | 144 | 660087 | 10108 | 11 |
| NAMC1-1 | sphalerite | 3 | 1865 | 224 | 659889 | 10176 | 17 |
| NAMC1-1 | sphalerite | 4 | 1741 | 166 | 661078 | 8953 | 7 |
| NAMC1-1 | sphalerite | 5 | 1699 | 155 | 660531 | 9689 | 7 |
| NAMC1-1 | sphalerite | 6 | 1755 | 188 | 661326 | 8661 | 4 |
| NAMC1-1 | sphalerite | 7 | 1844 | 145 | 659845 | 10293 | 7 |
| NAMC1-1 | sphalerite | 8 | 1755 | 188 | 661326 | 8661 | 4 |
| NAPA1-13 | sphalerite | 1 | 517 | 452 | 666201 | 4101 | 112 |
| NAPA1-13 | sphalerite | 2 | 544 | 445 | 665956 | 4358 | 111 |
| NAPA1-13 | sphalerite | 3 | 544 | 445 | 665956 | 4358 | 111 |
| NAPA1-13 | sphalerite | 5 | 570 | 465 | 665641 | 4646 | 148 |
| NAPA1-13 | sphalerite | 6 | 553 | 417 | 665790 | 4600 | 133 |
| NAPA1-13 | sphalerite | 7 | 541 | 435 | 665671 | 4708 | 151 |
| NAPA1-13 | sphalerite | 1 | 467 | 94 | 666365 | 4502 | 23 |
| NAPA1-13 | sphalerite | 2 | 568 | 307 | 665091 | 5477 | 189 |
| NAMC1-1 | sphalerite | 1 | 1352 | 125 | 662860 | 7453 | 7 |
| NAMC1-1 | sphalerite | 3 | 1442 | 123 | 662022 | 8370 | 4 |
| NAMC1-1 | sphalerite | 4 | 1346 | 129 | 661850 | 8744 | 4 |
| NAMC1-1 | sphalerite | 5 | 1496 | 129 | 662274 | 8018 | 9 |
| NAMC1-1 | sphalerite | 6 | 1479 | 125 | 662199 | 8085 | 9 |
| NAMC1-1 | sphalerite | 7 | 1475 | 105 | 662008 | 8376 | 12 |
| NAMC1-1 | sphalerite | 8 | 1557 | 127 | 662033 | 8162 | 14 |
| NAPA1-13 | sphalerite | 1 | 623 | 5 | 664420 | 6657 | |
| NAPA1-13 | sphalerite | 1 | 566 | 16 | 663126 | 8046 | 17 |
| NAPA1-13 | sphalerite | 2 | 511 | 5 | 663861 | 7404 | |
| NAPA1-13 | sphalerite | 3 | 429 | | 663536 | 7723 | 1 |
| NAPA1-13 | sphalerite | 1 | 500 | 363 | 665618 | 4766 | 140 |
| NAPA1-13 | sphalerite | 2 | 311 | 268 | 665200 | 5749 | 167 |
| NAPA1-13 | sphalerite | 3 | 544 | 332 | 665666 | 4745 | 133 |

| Sample ID | Mineral | FI# | Fe ppm | Cu ppm | Zn ppm | Cd ppm | Pb ppm |
|---|---|---|---|---|---|---|---|
| NAPA1-13 | sphalerite | 4 | 518 | 338 | 665564 | 4842 | 130 |
| NALD1-2 | sphalerite | 1 | 265 | 307 | 667090 | 3473 | 30 |
| NALD1-2 | sphalerite | 2 | 162 | 278 | 666524 | 4323 | 40 |
| NALD1-2 | sphalerite | 1 | 159 | 57 | 665675 | 4948 | 32 |
| NALD1-2 | sphalerite | 2 | 333 | 100 | 667144 | 3561 | 24 |
| NALD1-4 | sphalerite | 1 | 382 | 356 | 667060 | 3361 | 59 |
| NALD1-4 | sphalerite | 2 | 332 | 293 | 666623 | 3837 | 57 |
| NALD1-4 | sphalerite | 4 | 435 | 4 | 665713 | 5548 | 1 |
| NALD1-4 | sphalerite |  | 426 | 4 | 665988 | 5133 | 1 |
| NAPA1-13 | sphalerite | 1 | 375 | 4 | 664609 | 6754 | 3 |
| NAPA1-13 | sphalerite | 3 | 407 |  | 664621 | 6800 | 1 |
| NAPA1-13 | sphalerite | 1 | 289 | 79 | 666161 | 4910 | 16 |
| NAPA1-13 | sphalerite | 2 | 263 | 96 | 665933 | 5059 | 27 |
| NAPA1-13 | sphalerite | 4 | 229 | 103 | 664764 | 6550 | 28 |
| NAPA1-1 | sphalerite | 1 | 625 | 333 | 666446 | 3830 | 65 |
| NAPA1-1 | sphalerite | 3 | 650 | 339 | 666246 | 4006 | 71 |
| NAPA1-1 | sphalerite | 4 | 591 | 304 | 666107 | 4218 | 78 |
| NACP1-8 | sphalerite | 2 | 1164 | 3 | 663322 | 6970 |  |
| NACP1-8 | sphalerite | 3 | 1029 | 1 | 663220 | 7248 |  |
| NACP1-8 | sphalerite | 1 | 1081 | 51 | 665184 | 5041 | 2 |
| NACP1-8 | sphalerite | 2 | 1125 | 18 | 663600 | 6880 |  |
| NACP1-8 | sphalerite | 3 | 983 | 193 | 665959 | 3962 | 4 |
| NACP1-8 | sphalerite | 4 | 992 | 97 | 664345 | 5978 | 3 |
| NAEX1-2 | sphalerite | 1 | 806 | 214 | 665631 | 4319 | 76 |
| NAEX1-2 | sphalerite | 2 | 848 | 221 | 665575 | 4347 | 76 |
| NAEX1-2 | sphalerite | 3 | 734 | 181 | 665958 | 4131 | 63 |
| NAEX1-2 | sphalerite | 1 | 613 | 95 | 667214 | 3157 | 19 |
| NAEX1-2 | sphalerite | 2 | 597 | 72 | 667397 | 2964 | 9 |
| NAEX1-2 | sphalerite | 3 | 687 | 50 | 667248 | 3103 | 6 |
| NAEX1-2 | sphalerite | 1 | 649 |  | 664576 | 6246 |  |
| NAEX1-2 | sphalerite | 2 | 771 | 1 | 664903 | 5760 | 1 |
| NAEX1-2 | sphalerite | 3 | 785 | 2 | 664566 | 6122 |  |
| NAEX1-2 | sphalerite | 4 | 638 |  | 663978 | 6925 | 1 |
| NAEX1-7 | sphalerite | 1 | 1236 | 1 | 665058 | 4983 |  |
| NAEX1-7 | sphalerite | 2 | 990 |  | 664705 | 5669 |  |
| NAJP1-3 | sphalerite | 1 | 685 | 11 | 663111 | 7926 |  |
| NAJP1-3 | sphalerite | 2 | 562 | 22 | 662318 | 8913 | 1 |
| NALD1-4 | sphalerite | 7 | 414 | 5 | 666442 | 4426 | 1 |
| NALD1-4 | sphalerite | 8 | 368 | 8 | 665964 | 4963 | 6 |
| NALD1-4 | sphalerite | 9 | 397 | 12 | 666286 | 4572 | 8 |
| NALD1-4 | sphalerite | 10 | 393 | 14 | 665744 | 5137 | 5 |
| TSBS3-2 | sphalerite | 2 | 1489 | 497 | 665409 | 3982 | 25 |
| TSBS3-2 | sphalerite | 3 | 1393 | 621 | 665321 | 4054 | 21 |
| TSBS3-2 | sphalerite | 5 | 1715 | 308 | 663903 | 5675 | 31 |
| TSBS3-2 | sphalerite | 6 | 1421 | 610 | 666185 | 3017 | 9 |
| TSBS3-2 | sphalerite | 7 | 1337 | 704 | 666555 | 2614 | 4 |
| TSBS3-2 | sphalerite | 8 | 1095 | 733 | 667120 | 2243 | 2 |
| TSBS3-2 | sphalerite | 9 | 1277 | 605 | 666000 | 3451 | 14 |
| TSBS3-2 | sphalerite | 10 | 1588 | 375 | 665401 | 4031 | 16 |

| Sample ID | Mineral | FI# | Fe ppm | Cu ppm | Zn ppm | Cd ppm | Pb ppm |
|---|---|---|---|---|---|---|---|
| TSBS3-2 | sphalerite | 1 | 1360 | 236 | 667843 | 1661 | |
| TSBS3-2 | sphalerite | 2 | 1284 | 253 | 667846 | 1730 | |
| TSBS3-2 | sphalerite | 1 | 1289 | 246 | 667940 | 1628 | |
| TSBS3-2 | sphalerite | 2 | 1354 | 269 | 668126 | 1069 | |
| TSBS3-2 | sphalerite | 3 | 1371 | 196 | 668252 | 1197 | |
| TSBS3-2 | sphalerite | | 1201 | 229 | 668168 | 1487 | |
| TSBS3-2 | sphalerite | | 1664 | 654 | 667305 | 1419 | |
| TSNC1-1 | sphalerite | 4 | 816 | 966 | 667278 | 2047 | 3 |
| TSNC1-1 | sphalerite | 5 | 868 | 989 | 667570 | 1612 | 2 |
| TSNC1-1 | sphalerite | 6 | 893 | 1028 | 667439 | 1631 | 1 |
| TSNC1-1 | sphalerite | | 1318 | 166 | 666639 | 3184 | 4 |
| TSNC1-1 | sphalerite | | 941 | 649 | 668015 | 1494 | 1 |
| TSDW2-8 | sphalerite | 1 | 928 | 9 | 662288 | 8893 | |
| TSDW2-8 | sphalerite | 2 | 864 | 10 | 662949 | 8203 | 2 |
| TSDW2-8 | sphalerite | 1 | 1111 | 12 | 662047 | 8934 | 1 |
| TSDW2-8 | sphalerite | 2 | 1111 | 13 | 662109 | 8859 | 1 |
| TSDW2-8 | sphalerite | 1 | 1031 | 7 | 661943 | 9170 | 1 |
| TSDW2-8 | sphalerite | | 1496 | 68 | 659680 | 11140 | 3 |
| TSDW2-8 | sphalerite | 1 | 861 | 405 | 664916 | 4972 | 39 |
| TSDW2-8 | sphalerite | 1 | 890 | 5 | 663537 | 7409 | |
| TSDW2-8 | sphalerite | 1 | 765 | 505 | 665638 | 4599 | 45 |
| TSBS5-2 | sphalerite | 1 | 1297 | 147 | 665234 | 4530 | 4 |
| TSBS5-2 | sphalerite | 3 | 3031 | 3 | 663374 | 4889 | 1 |
| TSBS5-2 | sphalerite | 4 | 2879 | | 662735 | 5837 | 1 |
| TSCM2-1 | sphalerite | 2 | 1449 | 72 | 663199 | 6851 | 5 |
| TSCM2-1 | sphalerite | 3 | 1417 | 66 | 663324 | 6864 | 4 |
| TSCM2-1 | sphalerite | 4 | 1486 | 20 | 662625 | 7620 | 4 |
| TSCM2-1 | sphalerite | 1 | 1350 | 24 | 662627 | 7846 | 7 |
| TSCM2-1 | sphalerite | 2 | 1417 | 48 | 662284 | 8077 | 21 |
| TSCM2-1 | sphalerite | 4 | 1505 | 44 | 662731 | 7494 | 17 |
| TSCM2-1 | sphalerite | 1 | 1275 | 531 | 665764 | 3677 | 51 |
| TSCM2-1 | sphalerite | 2 | 1370 | 488 | 665669 | 3705 | 47 |
| TSCM2-1 | sphalerite | 3 | 1436 | 527 | 665611 | 3607 | 57 |
| TSDW2-8 | sphalerite | 1 | 1375 | 12 | 661358 | 9351 | |
| TSDW2-8 | sphalerite | 2 | 1438 | 11 | 660958 | 9729 | |
| TSDW2-8 | sphalerite | 3 | 1388 | 17 | 661122 | 9634 | |
| TSDW2-8 | sphalerite | | 1407 | 19 | 661810 | 8784 | |
| TSDW2-9 | sphalerite | 1 | 1349 | 2 | 662753 | 7649 | |
| TSDW2-9 | sphalerite | 2 | 1275 | 4 | 662872 | 7774 | 1 |
| TSDW2-9 | sphalerite | 3 | 1349 | 2 | 662753 | 7649 | |
| TSDW2-9 | sphalerite | 4 | 1342 | | 662859 | 7695 | 1 |
| TSDW2-9 | sphalerite | 5 | 1262 | 5 | 662924 | 7643 | 1 |
| TSDW2-9 | sphalerite | | 1334 | 3 | 662899 | 7629 | |
| TSGY2-3 | sphalerite | 1 | 1453 | 144 | 665591 | 4145 | 37 |
| TSGY2-3 | sphalerite | 2 | 1556 | 138 | 665901 | 3695 | 29 |
| TSGY2-3 | sphalerite | 3 | 1592 | 158 | 665429 | 4182 | 35 |
| TSPC2-1 | sphalerite | 1 | 2366 | 10 | 662042 | 7306 | 2 |
| TSPC2-1 | sphalerite | 2 | 2282 | 11 | 661974 | 7497 | 3 |
| TSPC2-1 | sphalerite | 4 | 2142 | 10 | 662248 | 7359 | 2 |

| Sample ID | Mineral | FI# | Fe ppm | Cu ppm | Zn ppm | Cd ppm | Pb ppm |
|---|---|---|---|---|---|---|---|
| TSPC2-1 | sphalerite | 5 | 2322 | 19 | 661828 | 7591 | 8 |
| TSPC2-1 | sphalerite | 6 | 2196 | 14 | 662050 | 7505 | 3 |
| TSPC2-1 | sphalerite | 1 | 1790 | 30 | 664485 | 5142 | 4 |
| TSPC2-1 | sphalerite | 6 | 1277 | 19 | 665120 | 5138 | 5 |
| TSOR2-3 | sphalerite | 1 | 2105 | 264 | 664844 | 4087 | 27 |
| TSOR2-3 | sphalerite | 2 | 2031 | 360 | 665302 | 3551 | 16 |
| TSPC2-1 | sphalerite | 1 | 1206 | 809 | 667472 | 1536 | 1 |
| TSPC2-1 | sphalerite | 2 | 1206 | 809 | 667472 | 1536 | 1 |
| TSPC2-1 | sphalerite | 3 | 721 | 558 | 666850 | 2720 | 16 |
| TSPC2-1 | sphalerite | 1 | 879 | 649 | 667652 | 1833 | 1 |
| TSPC2-1 | sphalerite | 2 | 1233 | 581 | 667325 | 1323 | 1 |
| TSPC2-1 | sphalerite | 1 | 2167 | 139 | 663479 | 5772 | 18 |
| TSPC2-1 | sphalerite | 2 | 2074 | 132 | 663258 | 6128 | 24 |
| TSPC2-1 | sphalerite | 3 | 2398 | 98 | 662184 | 7033 | 17 |
| TSTR1-7 | sphalerite | 1 | 1672 |  | 663209 | 6774 |  |
| TSTR1-7 | sphalerite | 3 | 1324 |  | 663294 | 7178 | 1 |
| TSTR1-7 | sphalerite | 4 | 1752 |  | 662759 | 7249 |  |
| TSTR1-7 | sphalerite | 5 | 1805 | 3 | 662975 | 6888 | 1 |
| TSTR1-7 | sphalerite | 6 | 2165 | 2 | 662021 | 7600 |  |
| TSTR1-7 | sphalerite | 7 | 1869 |  | 662684 | 7138 |  |
| TSTR1-7 | sphalerite | 8 | 2115 | 2 | 662493 | 7101 |  |
| TSTR1-7 | sphalerite | 9 | 1693 |  | 663279 | 6737 |  |
| TSTR1-7 | sphalerite | 10 | 1577 | 3 | 663337 | 6828 |  |
| TSTR1-7 | sphalerite | 11 | 1658 |  | 663082 | 7077 |  |
| TSTR1-7 | sphalerite | 12 | 1527 | 2 | 662868 | 7488 | 1 |
| TSWB3-9 | sphalerite | 1 | 1871 | 30 | 664353 | 5215 | 2 |
| TSWB3-9 | sphalerite | 2 | 1950 | 23 | 664498 | 4990 | 1 |
| TSWB3-9 | sphalerite | 6 | 1821 | 21 | 664313 | 5340 | 2 |
| TSWB3-9 | sphalerite | 8 | 1854 | 21 | 664471 | 5140 | 2 |
| TSWB3-9 | sphalerite | 9 | 1776 | 16 | 665052 | 4544 | 1 |
| TSWB3-9 | sphalerite | 12 | 1837 | 19 | 664530 | 5075 | 1 |
| TSBS5-2 | sphalerite | 1 | 1635 | 1 | 664313 | 5434 |  |
| TSBS5-2 | sphalerite | 2 | 1569 |  | 663407 | 6589 |  |
| TSBS5-2 | sphalerite | 1 | 1791 | 6 | 663379 | 6325 | 1 |
| TSBS5-2 | sphalerite | 2 | 1722 | 12 | 662997 | 6817 | 3 |
| TSBS5-2 | sphalerite | 3 | 1462 | 185 | 666263 | 2983 | 4 |
| TSBS5-2 | sphalerite | 1 | 1415 |  | 664061 | 6009 |  |
| TSBS5-2 | sphalerite | 2 | 1483 |  | 664511 | 5323 |  |
| TSBS5-2 | sphalerite | 3 | 1478 | 1 | 664979 | 4883 |  |
| TSBS5-2 | sphalerite | 4 | 1440 |  | 664450 | 5498 |  |
| TSBS5-2 | sphalerite | 5 | 1619 |  | 664047 | 5721 |  |
| TSBS5-2 | sphalerite | 1 | 1554 |  | 663657 | 6242 | 1 |
| TSBS5-2 | sphalerite | 2 | 1670 |  | 663328 | 6496 |  |
| TSBS5-2 | sphalerite | 3 | 1714 |  | 663393 | 6368 | 1 |
| TSBS5-2 | sphalerite | 4 | 1475 |  | 663448 | 6547 | 1 |
| TSBS5-2 | sphalerite | 5 | 1211 |  | 663526 | 6749 | 1 |
| TSBS5-2 | sphalerite | 6 | 1520 |  | 663934 | 6054 |  |
| TSCM2-1 | sphalerite | 1 | 2483 | 47 | 658067 | 11529 | 1 |
| TSCM2-1 | sphalerite | 2 | 1904 | 35 | 659311 | 10907 |  |

| Sample ID | Mineral | FI# | Fe ppm | Cu ppm | Zn ppm | Cd ppm | Pb ppm |
|---|---|---|---|---|---|---|---|
| TSCM2-1 | sphalerite | 3 | 2073 | 23 | 659812 | 10153 | |
| TSCM2-1 | sphalerite | 4 | 2697 | 76 | 657274 | 12274 | |
| TSCM2-1 | sphalerite | 5 | 2756 | 36 | 659205 | 9956 | |
| TSCM2-1 | sphalerite | 6 | 2551 | 30 | 659198 | 10283 | 1 |
| TSCM2-1 | sphalerite | 7 | 2624 | 32 | 659055 | 10268 | 1 |
| TSCM2-1 | sphalerite | 2 | 2597 | 33 | 658771 | 10595 | 1 |
| TSCM2-1 | sphalerite | 3 | 2362 | 7 | 659941 | 9592 | |
| TSCM2-1 | sphalerite | 4 | 2443 | 21 | 659773 | 9655 | 1 |
| TSCM2-1 | sphalerite | 1 | 2212 | 29 | 661933 | 7478 | 1 |
| TSCM2-1 | sphalerite | 3 | 2198 | 13 | 661496 | 7991 | |
| TSCM2-1 | sphalerite | 5 | 2291 | 19 | 660436 | 9080 | 1 |
| TSNC1-2 | sphalerite | 1 | 1496 | 38 | 665182 | 4496 | 2 |
| TSNC1-2 | sphalerite | 2 | 1471 | 34 | 665022 | 4670 | 2 |
| TSNC1-2 | sphalerite | 3 | 1462 | 40 | 665024 | 4684 | 2 |
| TSNC1-2 | sphalerite | 4 | 1429 | 35 | 665054 | 4734 | 3 |
| TSNC1-2 | sphalerite | 5 | 1341 | 32 | 664956 | 4911 | 2 |
| TSNC1-2 | sphalerite | 6 | 1447 | 21 | 664567 | 5275 | 1 |
| TSNC1-2 | sphalerite | 7 | 1463 | 22 | 665491 | 4272 | 1 |
| TSNC1-2 | sphalerite | 8 | 1378 | 18 | 665284 | 4547 | 1 |
| TSNC1-2 | sphalerite | 1 | 1343 | 282 | 665562 | 3820 | 34 |
| TSNC1-2 | sphalerite | 2 | 1157 | 299 | 665649 | 3919 | 34 |
| TSWB3-9 | sphalerite | 1 | 2226 | 137 | 661909 | 7232 | 33 |
| TSWB3-9 | sphalerite | 2 | 2378 | 131 | 661398 | 7654 | 36 |
| TSWB3-9 | sphalerite | 4 | 2371 | 144 | 661689 | 7322 | 31 |
| TSWB3-9 | sphalerite | 5 | 2310 | 135 | 661708 | 7368 | 33 |
| TSWB3-9 | sphalerite | 7 | 2165 | 131 | 662122 | 7058 | 33 |
| TSTR1-7 | sphalerite | 1 | 1952 | 2 | 662575 | 7112 | |
| TSTR1-7 | sphalerite | 2 | 1872 | 1 | 662480 | 7303 | |
| TSTR1-7 | sphalerite | 5 | 1808 | | 662225 | 7653 | |
| TSTR1-7 | sphalerite | 6 | 1691 | | 662778 | 7148 | 1 |
| TSTR1-7 | sphalerite | 7 | 1772 | | 662272 | 7682 | |
| TSTR1-7 | sphalerite | 8 | 1799 | | 662186 | 7709 | |
| TSTR1-7 | sphalerite | 9 | 1637 | | 662305 | 7787 | |
| TSTR1-7 | sphalerite | 10 | 1631 | | 662398 | 7641 | |
| TSTR1-7 | sphalerite | 11 | 1767 | | 663492 | 6379 | |
| TSTR1-7 | sphalerite | 12 | 1610 | | 663636 | 6423 | |
| TSTR1-7 | sphalerite | 13 | 1356 | 4 | 663506 | 6902 | 1 |
| TSTR1-7 | sphalerite | 14 | 1809 | | 663439 | 6396 | |
| TSTR1-7 | sphalerite | 15 | 1695 | | 663054 | 7022 | |
| TSTR1-7 | sphalerite | 17 | 1755 | | 662970 | 7054 | |
| TSWC1-3 | sphalerite | 1 | 2962 | | 660658 | 8062 | 1 |
| TSWC1-3 | sphalerite | 4 | 2746 | 3 | 661029 | 7912 | |
| TSWC1-3 | sphalerite | 5 | 2869 | | 660806 | 8010 | |
| TSWC1-3 | sphalerite | 8 | 2338 | | 661711 | 7658 | |
| 35_8V22 | sphalerite | 1 | 2072 | 6 | 660562 | 9212 | 10 |
| 35_8V22 | sphalerite | 2 | 601 | 67 | 665121 | 5751 | 9 |
| 35_8V22 | sphalerite | 1 | 15486 | 140 | 645969 | 6650 | 2893 |
| 35_8V22 | sphalerite | 1 | 2125 | 78 | 662039 | 6770 | 24 |
| 35_8V22 | sphalerite | | 2581 | 40 | 660382 | 8715 | 16 |

| Sample ID | Mineral | FI# | Fe ppm | Cu ppm | Zn ppm | Cd ppm | Pb ppm |
|---|---|---|---|---|---|---|---|
| 35_8V22 | sphalerite | 2 | 1916 | 41 | 662664 | 7040 | 15 |
| 35_8V22 | sphalerite | 3 | 2043 | 42 | 662926 | 6677 | 14 |
| WF2 | sphalerite | 1 | 1148 | 69 | 658900 | 12473 | 11 |
| WF2 | sphalerite | 3 | 813 | 93 | 665178 | 5234 | 24 |
| WF2 | sphalerite | 1 | 3053 | 6 | 652922 | 16836 | 30 |
| MAG13 | sphalerite | 1 | 253 | 13 | 665104 | 6239 | 1 |
| MAG13 | sphalerite | 3 | 295 | | 666313 | 4870 | 1 |
| MAG13 | sphalerite | 1 | 2911 | 358 | 660887 | 7439 | 38 |
| MAG13 | sphalerite | 1 | 743 | 24 | 667445 | 2819 | 1 |
| MAG13 | sphalerite | 2 | 620 | 204 | 667860 | 2117 | 1 |
| MAG13 | sphalerite | 3 | 993 | 134 | 667349 | 2114 | 1 |
| MAG13 | sphalerite | 4 | 1035 | 168 | 667382 | 2262 | 2 |
| MAG13 | sphalerite | 1 | 1828 | 129 | 665706 | 3131 | 1 |
| MAG13 | sphalerite | 2 | 3485 | 66 | 663797 | 3547 | |
| MAG13 | sphalerite | 1 | 708 | 211 | 667588 | 2459 | 3 |
| MAG13 | sphalerite | 2 | 825 | 155 | 667582 | 2496 | 2 |
| MAG13 | sphalerite | 3 | 1169 | 10 | 663679 | 6972 | 1 |
| VTSW2 | sphalerite | 1 | 5211 | 1659 | 647261 | 16715 | 1277 |
| MAG13C | sphalerite | 1 | 4432 | | 661387 | 5363 | |
| MAG13A | sphalerite | 1 | 4514 | 1 | 661202 | 5482 | |
| MAG13A | sphalerite | 2 | 4684 | | 661043 | 5399 | |
| MAG13A | sphalerite | 3 | 5039 | 5 | 660980 | 5025 | 2 |
| MAG13A | sphalerite | 4 | 5352 | | 660678 | 4998 | 1 |
| MAG13A | sphalerite | 5 | 4553 | 3 | 661526 | 5101 | 1 |
| MAG13A | sphalerite | 1 | 4006 | | 660986 | 6379 | 1 |
| MAG13A | sphalerite | 4 | 4258 | | 660633 | 6425 | 1 |
| MAG13B | sphalerite | 1 | 1875 | 174 | 666598 | 2145 | 2 |
| MAG13B | sphalerite | 2 | 3575 | 222 | 664343 | 2597 | |
| MAG13C | sphalerite | 1 | 10822 | 52 | 655355 | 4302 | 107 |
| VTSW2E | sphalerite | 1 | 2069 | 740 | 657842 | 11140 | 236 |
| VTSW2E | sphalerite | 4 | 3568 | 920 | 655275 | 11909 | 328 |
| VTSW2E | sphalerite | 1 | 2264 | 508 | 662454 | 5766 | 163 |
| WF2B | sphalerite | 1 | 1635 | 133 | 664144 | 5481 | 28 |
| WF2B | sphalerite | 2 | 1541 | 39 | 663842 | 6001 | 10 |
| WF2B | sphalerite | 3 | 1858 | 173 | 662709 | 6813 | 44 |
| WF2B | sphalerite | 4 | 1871 | 212 | 664104 | 5121 | 61 |